

# SAVER: Mitigating Hallucinations in Large Vision-Language Models via Style-Aware Visual Early Revision

Zhaoxu Li<sup>1,2</sup>, Chenqi Kong<sup>2\*</sup>, Yi Yu<sup>2</sup>, Qiangqiang Wu<sup>3</sup>, Xinghao Jiang<sup>4</sup>, Ngai-Man Cheung<sup>5</sup>, Bihan Wen<sup>2</sup>, Alex Kot<sup>2</sup>, Xudong Jiang<sup>2</sup>

<sup>1</sup>ROSE Lab, Interdisciplinary Graduate Programme, Nanyang Technological University, Singapore

<sup>2</sup>ROSE Lab, School of Electrical and Electronic Engineering, Nanyang Technological University, Singapore

<sup>3</sup>City University of Hong Kong, Hong Kong

<sup>4</sup>Shanghai Jiao Tong University, China

<sup>5</sup>Singapore University of Technology and Design, Singapore

{zhaoxu001, yuyi0010}@e.ntu.edu.sg, qiangqwu2-c@my.cityu.edu.hk, xhjiang@sjtu.edu.cn, ngaiman\_cheung@sutd.edu.sg, {chenqi.kong, bihan.wen, eackot, exdjiang}@ntu.edu.sg

## Abstract

Large Vision-Language Models (LVLMs) recently achieve significant breakthroughs in understanding complex visual-textual contexts. However, hallucination issues still limit their real-world applicability. Although previous mitigation methods effectively reduce hallucinations in photographic images, they largely overlook the potential risks posed by stylized images, which play crucial roles in critical scenarios such as game scene understanding, art education, and medical analysis. In this work, we first construct a dataset comprising photographic images and their corresponding stylized versions with carefully annotated caption labels. We then conduct head-to-head comparisons on both discriminative and generative tasks by benchmarking 13 advanced LVLMs on the collected datasets. Our findings reveal that stylized images tend to induce significantly more hallucinations than their photographic counterparts. To address this issue, we propose **Style-Aware Visual Early Revision (SAVER)**, a novel mechanism that dynamically adjusts LVLMs' final outputs based on the token-level visual attention patterns, leveraging early-layer feedback to mitigate hallucinations caused by stylized images. Extensive experiments demonstrate that SAVER achieves state-of-the-art performance in hallucination mitigation across various models, datasets, and tasks.

## Introduction

Large Vision-Language Models (LVLMs) (OpenAI 2023; Chen et al. 2023; Yin et al. 2024a; Zhao et al. 2024; Zhang et al. 2024b) have achieved remarkable successes in a plethora of applications in the past few years (Li et al. 2022; Liu et al. 2023a; Zhu et al. 2023). However, the phenomenon of hallucination can cause severe consequences in some practical scenarios, such as medical analyzes (Hu et al. 2023; Wang et al. 2023b), autonomous driving (Chen et al. 2024b; Liu et al. 2023b), and human-computer interaction (Brie et al. 2023). These issues raise pressing security concerns and may cause unintended harm to the public, significantly hindering the real-world deployment of LVLMs.

To mitigate hallucinations, existing approaches can be broadly categorized into two groups: instruction tuning

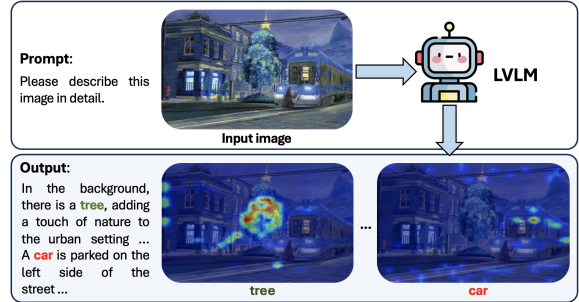


Figure 1: Correlation map between image tokens and generated tokens. Red: hallucinated tokens, showing sparse, low-confidence correlations. Green: real tokens, showing concentrated clusters over the corresponding regions.

methods (Sun et al. 2023; Xing et al. 2024) and decoding-based methods (Chuang et al. 2023; Jiang et al. 2024). The former requires retraining LVLMs using curated datasets and tuning strategies, which effectively reduce hallucinations while introducing expensive computational costs. The latter employs post-hoc correction mechanisms, adjusting logit scores at each generative step to encourage LVLMs to focus more on the corresponding visual content. While these methods have shown promising results for photographic images, they suffer from significant performance drops when applied to stylized images (e.g., game and sketch).

Stylized images play a critical role in various applications, including art education, medical analysis, and criminal forensics. For instance, LVLMs can interpret forensic sketches to retrieve matches from photographic databases or generate suspect profiles. Minimizing hallucinations in such scenarios is essential to enhance the reliability of these models. However, a comprehensive benchmark for assessing LVLM performance on stylized images remains unavailable. To fill this gap, we construct a dataset comprising paired captions and both photographic and style-transferred images generated using state-of-the-art methods across five stylistic domains. We evaluate 13 advanced LVLMs and observe

\*Corresponding author

that stylized images significantly increase hallucination rates compared to their original photographic counterparts.

To investigate the underlying causes, we conduct an empirical analysis by measuring the correlations between stylized image representations and the generated tokens. Fig. 1 visualizes the representational patterns of real and hallucinated objects in stylized images. We observe that real object representations exhibit concentrated, high-confidence activation regions, while the hallucinated object displays sparse, low-confidence distributions. This insight naturally inspires the design of a decoding strategy that encourages the model to focus more precisely on the relevant visual regions.

We propose **SAVER**: Style-Aware Visual Early Revision, a training-free hallucination mitigation strategy designed to address hallucination issues in stylized images. Due to the strong knowledge priors of language models, LVLMs tend to progressively suppress visual information in later model layers (Wang et al. 2024a; Jiang et al. 2024). To counteract this, SAVER dynamically searches the optimal preceding layers with highly concentrated representational patterns to refine the output token logits. As a plug-and-play decoding strategy, SAVER can be seamlessly integrated into various LVLMs and significantly reduces hallucination rates for stylized images without requiring additional training.

Our key contributions are: (1) To the best of our knowledge, we are the first to construct a captioning dataset specifically for stylized images. We further establish a benchmark using 13 advanced LVLMs and find that stylized images tend to produce more hallucinations; (2) Compared to hallucinated tokens, we demonstrate that the correlation patterns between correct tokens and input visual contents exhibit denser visual activations in early layers. Based on this insight, we propose SAVER, a training-free decoding strategy that dynamically corrects generated tokens by leveraging high-confidence activations from earlier layers; (3) Extensive experimental results show that SAVER consistently outperforms previous methods, effectively mitigating hallucinations across a variety of models, datasets, and tasks.

## Related Work

**Large Vision-Language Models (LVLMs).** Large Language Models (LLMs) such as LLaMA (Touvron et al. 2023) and Vicuna (Chiang and Li 2 May 2025) have achieved remarkable advancements. The rapid development of LVLMs has significantly enhanced the ability of foundation models to interpret and reason about visual content. Early LVLMs, including BLIP (Li et al. 2022) and LLaVA (Liu et al. 2023a), extended LLMs to handle image understanding and reasoning tasks. To bridge the modality gap between vision and language, various approaches have been adopted, such as linear projection layers (e.g., LLaVA (Liu et al. 2023a), MiniGPT-4 (Zhu et al. 2023)), Q-former modules (e.g., BLIP-2 (Li et al. 2023a), InstructBLIP (Dai et al. 2023)), and cross-attention mechanisms (e.g., Flamingo (Alayrac et al. 2022), OpenFlamingo (Awadalla et al. 2023)). More recent models, such as GPT-4o (OpenAI 2023) and Gemini (AI 2024), have demonstrated exceptional capabilities in visual reasoning and understanding. Nevertheless, despite these advancements, hallucination remains a significant challenge.

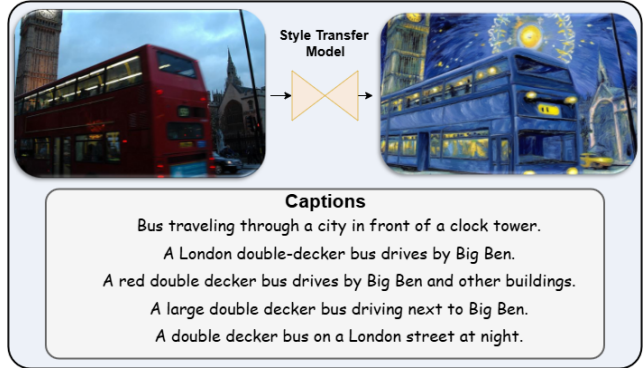


Figure 2: Top left: original image; top right: stylized image; bottom: COCO captions listing all salient objects.

**Visual Hallucination in LVLMs** typically refers to cases where the generated text is inconsistent with the input image at the instance level (Rohrbach et al. 2018; Zhou et al. 2023; Li et al. 2023b; Guan et al. 2024) or the faithfulness of the generated free-form answer (Jing et al. 2023). There are various potential factors that can cause hallucinations, including modality gap, training data bias, error accumulation, etc. (Zhou et al. 2023). To evaluate LVLM hallucination levels, CHAIR (Rohrbach et al. 2018) proposes measuring object hallucination rates in output captions. The POPE benchmark (Li et al. 2023b) assesses object hallucinations using binary “Yes/No” questions. Additionally, MME (Fu et al. 2024) provides a more challenging dataset for hallucination evaluation, which encompasses various hallucination types, such as object, attribute, counting, etc. AMBER (Wang et al. 2023a) supports both generative and discriminative tasks, covering existence, attribute, and relation hallucinations. While prior works have primarily focused on natural photographic images, this study constructs a new dataset and comprehensive benchmark to investigate hallucination in LVLMs when processing stylized images.

**Hallucination Mitigation.** Existing methods fall into tuning-based and decoding-based categories. Tuning-based approaches curate specialized datasets (Wang et al. 2024c; Zhang et al. 2024a; Yang et al. 2024; Chen et al. 2024a; Yue, Zhang, and Jin 2024; Jing and Du 2024) and apply alignment training (Xie et al. 2024; Sun et al. 2023; Xing et al. 2024; Yu et al. 2025), but are costly in annotation and computation. In contrast, training-free methods (Yin et al. 2024b) and decoding-based techniques (Huang et al. 2024; An et al. 2024) are more efficient. Recent contrastive decoding methods (Leng et al. 2024; Chen et al. 2024d; Chuang et al. 2023; Zhuang et al. 2024; Suo et al. 2025) further enhance performance by leveraging visual comparisons. Deco (Wang et al. 2024a) and Attention Lens (Jiang et al. 2024) emphasize layer selection to mitigate hallucination. Our method, **SAVER**, differs from these two approaches by dynamically selecting non-hallucinated tokens without the need to train a detector. And SAVER leverages richer visual signals during layer selection for final output revision, thereby achieving better hallucination mitigation performance.

## Benchmarking Stylized Image Hallucination

In this section, we introduce our proposed style dataset by outlining its motivation, construction process, and image generation pipeline. We then present the benchmark along with a detailed description of the procedures. An example style image from the dataset is shown in Fig. 2.

**Motivation.** We propose this dataset to examine object hallucination in cross-style scenarios, evaluating LVLMs’ ability to analyze images from diverse domains. This section describes the construction of our style-diverse dataset and benchmark. Existing LVLM benchmarks mainly use photographic (“Original”) images, reflecting their dominance in real-world applications. However, images also come in styles like Cartoon and Sketch, where objects may appear visually distinct (e.g., a cat with unusual colors). As shown in Fig. 2, such variations pose challenges for LVLMs, which may lack exposure to these styles during training. To address this, we introduce a framework to assess hallucination behaviors across a range of artistic styles.

**Dataset.** Follow previous hallucination works (Rohrbach et al. 2018; Li et al. 2023b), we sampled images from the COCO dataset to construct a high-quality stylized dataset. Each selected image contains at least five annotated objects to create a challenging evaluation setting. We applied SOTA InstantStyle (Wang et al. 2024b) model to generate style-transferred images in five styles: Cartoon, Game, Graffiti, Painting, and Sketch, ending up with 1,800 images. We carefully checked each pair of images and manually filter out the low-quality one, ensuring that each original image and its stylized versions share identical annotations, including object and caption labels.

**Benchmark.** We construct a benchmark using two metrics:

- **CHAIR:** Caption Hallucination Assessment with Image Relevance (CHAIR) (Rohrbach et al. 2018) measures the proportion of hallucinated objects—those mentioned in the caption but absent in the image. We use two variants: CHAIR<sub>i</sub> (instance-level) and CHAIR<sub>s</sub> (sentence-level), defined as:

$$\begin{aligned} \text{CHAIR}_i &= \frac{\{\text{hallucinated instances}\}}{\{\text{all mentioned instances}\}}, \\ \text{CHAIR}_s &= \frac{\{\text{captions with hallucinations}\}}{\{\text{all captions}\}}. \end{aligned} \quad (1)$$

- **POPE:** Polling-based Object Probing Evaluation (POPE) (Li et al. 2023b) evaluates hallucination by asking LVLMs “Yes/No” questions about object presence, using three negative sampling strategies: random, popular (top- $k$  frequent absent objects), and adversarial (top- $k$  absent objects ranked by co-occurrence with ground-truth). We follow the original POPE settings and generate 6 questions for each image, resulting in  $1800 \times 6 \times 3$  question image pairs.

## Style Aware Visual Early Revision

We conduct a comprehensive benchmark and study to uncover the underlying mechanisms that lead to object hallucination when processing stylized images. Guided by these

findings, we propose **Style-Aware Visual Early Revision (SAVER)**, a novel inference-time strategy aimed at reducing hallucinations caused by style-transferred content. The overall design and workflow of SAVER are illustrated in Fig. 3.

## Preliminaries

LVLMs for text generation typically consist of three key components: a vision encoder, a projection module, and an autoregressive language model. The vision encoder first converts an input image into a sequence of visual tokens  $X_V = \{x_{v_1}, x_{v_2}, \dots, x_{v_P}\}$ . In parallel, a text prompt is tokenized into  $Q$  textual tokens  $X_C = \{x_{c_1}, x_{c_2}, \dots, x_{c_Q}\}$ . Here  $P$  and  $Q$  are the lengths of the visual and textual tokens. The visual and textual embeddings are concatenated to form the model input  $X$ , which is passed through an autoregressive language model composed of  $N$  stacked transformer decoder layers. At each layer  $i$ , the model produces hidden states  $h^i = \{h_0^i, h_1^i, \dots, h_{T-1}^i\}$ , where  $T = P + Q$ ,  $P$  is the length of the visual tokens. During generation, the hidden state at the final position  $h_{T-1}^N$  is projected via an affine transformation  $\phi(\cdot)$ , typically using an unembedding matrix  $W_U \in \mathbb{R}^{|V| \times d}$ , to produce a logit distribution over the vocabulary  $V$ .

## Stylization Amplifies Object Hallucination

We investigate the impact of image stylization on object hallucination in LVLMs, specifically in the context of image captioning. Our benchmark includes various LVLMs, covering both open-source models (e.g., LLaVA (Liu et al. 2024b), MiniGPT-4 (Zhu et al. 2023), InstructBLIP (Dai et al. 2023), TinyLLaVA (Zhou et al. 2024), Phi-3-V (Abdin et al. 2024), Fuyu (Bavishi et al. 2023), Idefics2 (Laurençon et al. 2024), mPLUG-Owl2 (Ye et al. 2024), Qwen-VL (Bai et al. 2023)) and closed-source platforms (e.g., GPT-4o (OpenAI 2023), Gemini-1.5-Pro (AI 2024)).

To elicit diverse responses, we employ two prompt templates: a detailed prompt (“Please describe this image in detail”) and a concise prompt (“Provide a one-sentence caption for the provided image.”). The generated captions are evaluated using the CHAIR metric, with results summarized in Tab. 1 and Tab. 7 (Appendix). In addition, we assess hallucination across three splits of the Style-POPE benchmark, with detailed results visualized in Fig. 5 in the Appendix.

Our experiments reveal a consistent increase in object hallucination when models process stylized images, such as those rendered in Cartoon, Game, Graffiti, Painting, and Sketch styles, compared to original photographs. This performance degradation highlights the models’ reduced grounding capabilities under stylistic shifts.

## Visual Sensitivity with Style-Aware Score (SAS)

To quantify the influence of visual style on token generation, we propose **Style-Aware Score (SAS)**, which measures the alignment between intermediate visual representations and the final output tokens. Specifically, SAS captures the contribution of early-layer visual embeddings to token prediction by analyzing the intermediate hidden states within the transformer decoder. Given a set of candidate tokens selected

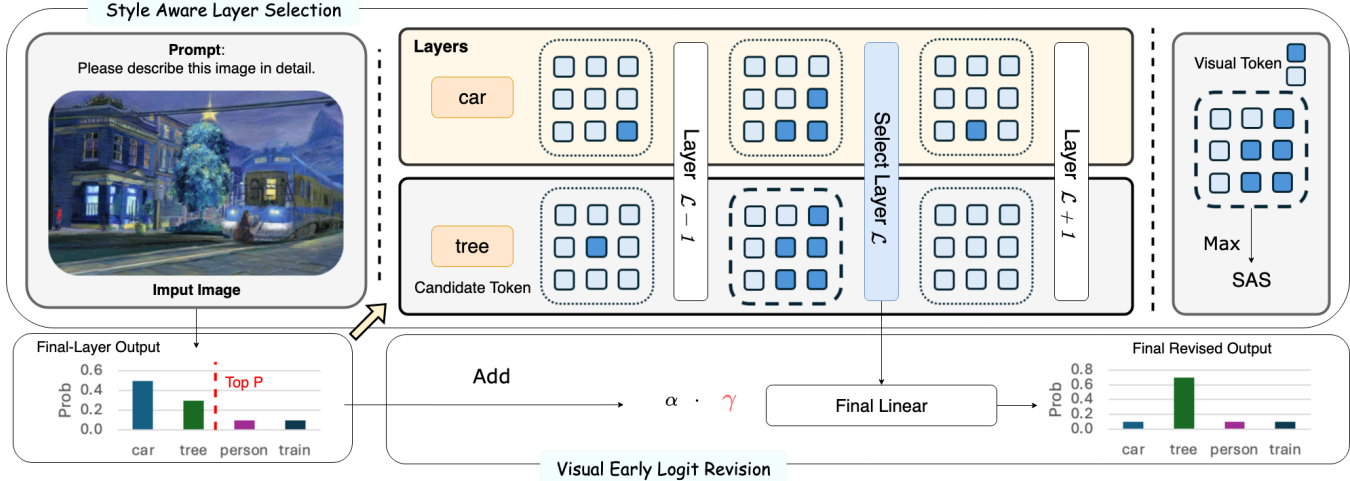


Figure 3: Framework of SAVER. SAVER first selects the top- $p$  candidate tokens, then selects an appropriate layer from the preceding layers based on Style-Aware Score, and finally, revise the final layer output.

Table 1: Style-Chair Benchmark with prompt: “Please describe this image in detail”. Lower indicate fewer hallucinations.

| Model                 | Cartoon |      | Game |      | Graffiti |      | Painting |      | Sketch |      | Original |      | Average |      |
|-----------------------|---------|------|------|------|----------|------|----------|------|--------|------|----------|------|---------|------|
|                       | Ci      | Cs   | Ci   | Cs   | Ci       | Cs   | Ci       | Cs   | Ci     | Cs   | Ci       | Cs   | Ci      | Cs   |
| GPT4o                 | 10.3    | 29.0 | 7.5  | 23.0 | 7.9      | 21.3 | 6.7      | 20.0 | 5.6    | 17.7 | 4.7      | 16.7 | 7.1     | 21.3 |
| Gemini-1.5-PRO        | 13.5    | 25.3 | 7.9  | 14.3 | 13.1     | 18.7 | 11.3     | 19.3 | 7.0    | 13.3 | 6.2      | 18.3 | 9.8     | 18.2 |
| LLaVA-1.5             | 12.0    | 43.3 | 9.1  | 31.7 | 11.4     | 37.7 | 11.2     | 34.7 | 11.4   | 37.7 | 6.8      | 26.7 | 10.3    | 35.3 |
| LLaVA-1.5-13b         | 10.7    | 38.7 | 10.3 | 35.0 | 11.0     | 37.3 | 9.6      | 33.3 | 10.0   | 31.7 | 7.4      | 27.3 | 9.8     | 33.9 |
| LLaVA-v1.6-mistral-7b | 10.9    | 25.7 | 8.8  | 22.0 | 9.9      | 24.0 | 10.4     | 26.7 | 10.1   | 25.7 | 6.0      | 19.3 | 9.4     | 23.9 |
| InstructBLIP          | 13.7    | 45.0 | 9.4  | 36.7 | 12.0     | 37.3 | 8.9      | 31.7 | 10.2   | 35.7 | 6.6      | 25.0 | 10.1    | 35.2 |
| MiniGPT-4             | 12.0    | 38.7 | 9.8  | 33.0 | 11.3     | 34.7 | 10.6     | 32.7 | 11.3   | 33.3 | 8.8      | 31.0 | 10.6    | 33.9 |
| Tinyllava             | 13.6    | 34.0 | 8.1  | 20.3 | 9.3      | 22.0 | 10.4     | 24.0 | 9.2    | 22.3 | 6.5      | 19.0 | 9.5     | 23.6 |
| Phi3V                 | 11.3    | 27.3 | 9.8  | 25.7 | 11.3     | 20.7 | 9.6      | 26.7 | 9.8    | 25.7 | 6.8      | 22.3 | 9.8     | 24.7 |
| Fuyu                  | 17.7    | 60.3 | 17.1 | 60.7 | 24.7     | 61.3 | 17.7     | 55.0 | 19.8   | 57.7 | 10.8     | 48.7 | 18.0    | 57.3 |
| Idefics2-8b           | 9.5     | 23.7 | 8.6  | 23.3 | 9.9      | 24.7 | 11.4     | 31.7 | 9.2    | 26.0 | 6.5      | 20.0 | 9.2     | 24.9 |
| mPLUG-Owl2            | 13.5    | 40.7 | 11.6 | 37   | 17.2     | 44.7 | 13.9     | 38.7 | 10.4   | 35   | 7.9      | 27.3 | 12.4    | 37.2 |
| Qwen-VL               | 13.2    | 42.7 | 8.3  | 30.3 | 14.8     | 39.3 | 10.2     | 30.7 | 10.2   | 35.0 | 5.0      | 19.7 | 10.3    | 33.0 |

from the final decoder layer’s logits, we compute the SAS by aggregating token logits across visual token positions and selected intermediate layers. Let  $\mathcal{L} \subset \{1, 2, \dots, N-1\}$  denote a predefined set of candidate transformer layers (e.g., early or deep layers). For each selected layers  $l \in \mathcal{L}$ , we extract logits  $\mathbf{Z}_l \in \mathbb{R}^{T \times |V|}$  by projecting the hidden states  $h^l$  via the output embedding matrix  $W_U$ , i.e.,  $\mathbf{Z}_l = W_U h^l$ . We then isolate the logits corresponding to the visual token positions, yielding  $\mathbf{Z}_l^{(v)} \in \mathbb{R}^{P \times |V|}$ . The Style-Aware Score for a candidate token  $c$  at layer  $l$  is defined as:

$$\text{SAS}_l(c) = \sum_{p=1}^P \text{softmax}(\mathbf{Z}_l^{(v)}(c)) \quad (2)$$

Where  $P$  is the visual token length. This score quantifies the model’s reliance on visual features during token generation. **A higher SAS implies stronger alignment between visual input and the generated token, indicating stronger grounding.** SAS provides a way to quantitatively assess a model’s sensitivity to visual inputs.

## Reduced Style Awareness Produces Hallucination

Prior studies have shown that language model priors often dominate visual inputs, with attention skewed toward object-like tokens (Wang et al. 2024a; Jiang et al. 2024). Motivated by these findings, we hypothesize that intermediate representations in early decoder layers encode varying degrees of visual awareness, which directly influences hallucination. Fig. 1 illustrates this hypothesis: tokens grounded in real visual objects (e.g., “tree”) exhibit higher visual awareness, while hallucinated tokens show weaker spatial alignment. To empirically validate this observation, we conduct a layer-wise analysis of SAS trajectories throughout the transformer stack. In the Style-POPE benchmark, each image is paired with six object existence questions (e.g., “Is there a bottle in the image?”). A “no” label indicates the object is not present. For each question, we compute the average SAS values based on the predicted answer and the queried object. As shown in Fig. 4, tokens corresponding to real objects consistently exhibit significantly higher SAS scores than those associated with non-existent (hallucinated) ob-

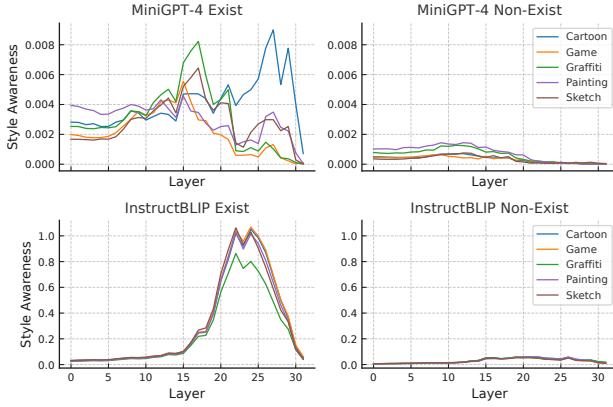


Figure 4: Statistics evaluation of style awareness. The top results are evaluated on MiniGPT-4, and the bottom results are evaluated on InstructBLIP. SAS curves for real objects consistently lie above those for hallucinated objects.

---

**Algorithm 1: Style-Aware Visual Early Revision (SAVER)**

---

**Require** Input IDs  $\mathbf{x}$ , beam width  $B$ , early layers  $\mathcal{L}$ , thresholds  $k, p$ , scale  $\alpha$

**Initialize beams**  $\{\mathbf{x}^{(b)}\}_{b=1}^B$

- 1: **while** condition **do**
- 2:   **Decode:** Forward decoder to get final-layer logits  $\mathbf{z}_t^N$  and early-layer logits  $\{\mathbf{z}_t^l\}_{l \in \mathcal{L}}$
- 3:   **if** first decoding step **then**
- 4:     **Precompute SAS:** cache  $\{\text{SAS}_l(c)\}_{l \in \mathcal{L}, c \in V}$
- 5:   **end if**
- 6:   **Candidate Filtering:**  $\mathcal{C}_t \leftarrow \text{TOPK/TOPP}(\mathbf{z}_t^N, k, p)$
- 7:   **Style-Confidence Layer Selection:**
- 8:      $\gamma = \max_{l \in \mathcal{L}, c \in \mathcal{C}_t} \text{SAS}_l(c)$
- 9:      $l^* = \arg \max_{l \in \mathcal{L}} \max_{c \in \mathcal{C}_t} \text{SAS}_l(c)$
- 10:   **Logit Revision:**  $\hat{\mathbf{z}}_t = \mathbf{z}_t^N + \alpha \cdot \gamma \cdot (\mathbf{z}_t^{l^*} \odot \mathbf{m}_t)$ , where  $\mathbf{m}_t$  masks  $\mathcal{C}_t$
- 11:   **Beam Update:** Update beams using revised logits  $\hat{\mathbf{z}}_t$
- 12: **end while**
- 13: **return** best completed beam(s)

---

jects, especially in the early layers. We further observe that SAS distributions are style-dependent, with peaks often occurring in earlier layers of the model.

## Our Method

As discussed in the previous section, object hallucination in stylized images arises from the model’s neglect of the corresponding visual patterns during decoding. To mitigate this issue, we propose **Style-Aware Visual Early Revision (SAVER)**, a test-time strategy that adjusts final predictions using early-layer representations. Notably, SAVER introduces no additional learnable parameters and can be seamlessly integrated into existing LVLMs and mitigate hallucination problems. SAVER operates during decoding and consists of three key steps: (1) identifying a candidate set of plausible tokens using top- $p$  filtering; (2) selecting the most

visually grounded layer via the Style-Aware Score (SAS); and (3) revising the logits to better reflect visual evidence from that layer. The algorithm pipeline is presented in **Algorithm 1**, which outlines the step-by-step implementation of SAVER at test time.

**Style-Aware Layer Selection.** Our previous analysis shows that correct tokens are highly correlated with the activation regions in early layers where visual features dominate. In this vein, we define a candidate set of transformer layers  $\mathcal{L} \subset \{1, \dots, N-1\}$  and identify a candidate token set  $\mathcal{C}_t$  by applying top- $p$  filtering to the final-layer logits  $\mathbf{z}_t^N \in \mathbb{R}^{|V|}$  and top- $k$  for the tokens. For each layer  $l \in \mathcal{L}$ , we compute a style-confidence score based on the maximum Style-Aware Score (SAS; see Eq. (2)) among the candidate tokens:

$$l^* = \arg \max_{l \in \mathcal{L}} \sigma_l, \quad \gamma = \sigma_{l^*}, \quad \text{where} \quad \sigma_l = \max_{c \in \mathcal{C}_t} \text{SAS}_l(c). \quad (3)$$

Here,  $\gamma \in [0, 1]$  quantifies the influence of stylistic features at the selected layer  $l^*$ . This mechanism allows SAVER to dynamically identify which layer provides the most relevant visual grounding at each decoding step, balancing between overfitting to style and ignoring visual context. The use of maximum SAS ensures that even if a single token strongly activates visual features at a certain layer, that signal is preserved in layer selection. In practice, we find that this adaptive grounding depth is critical for generalization across diverse styles and model architectures.

**Logit Revision.** SAVER refines the final-layer logits  $\mathbf{z}_t^N$  by incorporating evidence from the selected style-sensitive layer  $l^*$ . Let  $\mathbf{m}_t \in \{0, 1\}^{|V|}$  denote a binary mask that activates only the candidate tokens in  $\mathcal{C}_t$ . The revised logits  $\hat{\mathbf{z}}_t$  are computed as:

$$\hat{\mathbf{z}}_t = \mathbf{z}_t^N + \alpha \cdot \gamma \cdot (\mathbf{z}_t^{l^*} \odot \mathbf{m}_t), \quad (4)$$

where  $\alpha$  is a scalar hyperparameter and  $\odot$  is element-wise multiplication. This formulation selectively amplifies predictions that are grounded in style-aware visual evidence, while suppressing tokens that may arise solely due to stylistic noise. By scaling with both  $\alpha$  and the layer-specific confidence  $\gamma$ , the method modulates its correction strength based on how strongly the model attends to visual input at  $l^*$ . Since SAVER operates per decoding step, it enables fine-grained correction without modifying the backbone model or compromising generation fluency. This makes it applicable in real-world scenarios with diverse data distributions, and effective even under domain shifts.

## Experiments

### Implementation Details

**Evaluation Models and Settings.** We evaluate our proposed method and baseline approaches on four representative LVLMs: InstructBLIP (Dai et al. 2023), MiniGPT-4 (Zhu et al. 2023), and LLaVA-1.5 (Liu et al. 2024b), LLaVA-1.6 (Liu et al. 2024a). The maximum length of the generated sequence is set to 64 tokens, with a repetition penalty of 1.0. Unless otherwise specified, decoding is performed using a fixed temperature of 0 and top- $k$ =1. For

Table 2: CHAIR hallucination evaluation results. Lower scores indicate fewer hallucinations. The best value is bolded, and the second best value is underlined.

| Model        | Method      | Cartoon     |             | Game       |             | Graffiti    |             | Painting    |             | Sketch      |             | Original   |             | Average    |             |
|--------------|-------------|-------------|-------------|------------|-------------|-------------|-------------|-------------|-------------|-------------|-------------|------------|-------------|------------|-------------|
|              |             | Ci          | Cs          | Ci         | Cs          | Ci          | Cs          | Ci          | Cs          | Ci          | Cs          | Ci         | Cs          | Ci         | Cs          |
| InstructBLIP | Greedy      | 13.7        | 45.0        | 9.4        | 36.7        | 12.0        | 37.3        | 8.9         | 31.7        | 10.2        | 35.7        | 6.6        | 25.0        | 10.1       | 35.2        |
|              | Beam        | 11.8        | 41.3        | 9.7        | 34.0        | 10.8        | 34.7        | <u>7.8</u>  | 27.3        | 10.4        | 38.3        | 7.1        | 28.7        | 9.6        | 34.1        |
|              | Dola        | 18.8        | 42.7        | 19.3       | 48.3        | 20.2        | 46.3        | <u>17.8</u> | 43.7        | 17.6        | 43.7        | 12.7       | 39.0        | 17.7       | 44.0        |
|              | OPERA       | 12.4        | 38.3        | 10.7       | 35.0        | 12.2        | 37.3        | 8.8         | 31.0        | 9.9         | 34.7        | 7.0        | 25.7        | 10.2       | 33.7        |
|              | Deco        | 10.9        | 36.3        | 8.9        | <b>28.0</b> | 10.6        | 30.7        | 9.4         | 26.0        | 8.2         | <b>25.3</b> | 5.5        | 22.3        | 8.9        | 28.1        |
|              | AGLA        | 12.4        | 41.0        | 9.6        | 36.0        | 12.8        | 38.0        | 9.9         | 33.0        | 10.4        | 37.7        | 7.0        | 27.3        | 10.4       | 35.5        |
| LLaVA-1.5    | SAVER(Ours) | <b>9.9</b>  | <b>32.0</b> | <b>8.0</b> | 30.0        | <b>9.9</b>  | <b>28.0</b> | <b>7.4</b>  | <b>25.3</b> | <b>7.8</b>  | <u>27.0</u> | <b>5.3</b> | <b>21.3</b> | <b>8.1</b> | <b>27.3</b> |
|              | Greedy      | 12.0        | 43.3        | 9.1        | 31.7        | <b>11.4</b> | 37.7        | 11.2        | 34.7        | 11.4        | 37.7        | 6.8        | 26.7        | 10.3       | 35.3        |
|              | Beam        | 11.5        | 39.3        | 9.3        | 32.3        | <u>11.9</u> | 33.3        | 10.2        | 34.3        | <u>10.5</u> | 36.7        | 6.0        | <b>24.0</b> | 9.9        | 33.3        |
|              | Dola        | 15.4        | 44.0        | 14.1       | 43.0        | <u>16.9</u> | 49.0        | 14.7        | 42.0        | <u>14.9</u> | 46.7        | 10.6       | <b>35.7</b> | 14.4       | 43.4        |
|              | OPERA       | 12.1        | 38.7        | 9.6        | 33.0        | 12.4        | 35.7        | 10.1        | 31.7        | 10.7        | <u>31.7</u> | <b>5.8</b> | 24.7        | 10.1       | 32.6        |
|              | Deco        | <b>11.2</b> | <b>31.3</b> | <b>8.9</b> | <u>30.0</u> | <u>11.9</u> | <u>32.7</u> | <u>9.4</u>  | <u>31.3</u> | <b>9.4</b>  | <b>30.7</b> | <b>5.9</b> | <b>21.3</b> | <b>9.5</b> | <b>29.6</b> |
|              | AGLA        | 11.3        | 38.0        | 9.3        | 31.3        | 12.5        | 40.0        | 10.4        | 33.3        | 11.9        | 39.3        | 6.7        | 26.7        | 10.4       | 34.8        |
| LLaVA-1.6    | SAVER(Ours) | <b>11.2</b> | <u>32.7</u> | <b>8.8</b> | <b>29.7</b> | <b>11.4</b> | <b>30.3</b> | <b>9.3</b>  | <b>29.0</b> | 10.6        | 32.0        | 6.6        | 26.0        | <u>9.7</u> | <u>30.0</u> |
|              | Greedy      | 12.3        | 27.0        | 8.8        | 22.0        | 9.9         | 24.0        | 10.4        | 26.7        | 10.1        | 25.7        | 6.0        | 19.3        | 9.4        | 23.9        |
|              | Beam        | 11.9        | 29.0        | 9.6        | 24.3        | <u>10.1</u> | 22.7        | 10.7        | 26.7        | 9.3         | 25.3        | 5.9        | 18.0        | 9.6        | 24.3        |
|              | Dola        | 13.6        | 31.0        | <u>8.1</u> | <b>18.3</b> | 10.2        | <b>17.7</b> | <u>8.9</u>  | <b>18.7</b> | 8.7         | 20.0        | <b>5.1</b> | <b>12.7</b> | <u>9.1</u> | <b>19.7</b> |
|              | OPERA       | <b>10.1</b> | <b>23.0</b> | <u>8.6</u> | <u>21.5</u> | 12.1        | 27.1        | 9.8         | 25.6        | <u>9.2</u>  | 24.7        | 6.0        | 17.4        | <u>9.3</u> | 23.2        |
|              | Deco        | 12.8        | 30.3        | 9.7        | 24.3        | 10.9        | 25.3        | <b>8.4</b>  | 22.0        | 9.3         | 26.7        | 6.1        | 18.7        | 9.5        | 24.6        |
| MiniGPT-4    | AGLA        | <u>10.8</u> | 28.0        | 9.2        | 23.3        | <u>9.9</u>  | 24.0        | 10.5        | 27.3        | 8.9         | 25.7        | 6.0        | 20.3        | 9.2        | 24.8        |
|              | SAVER(Ours) | 13.0        | 31.7        | <b>7.4</b> | <b>16.3</b> | <b>9.7</b>  | <u>20.3</u> | 9.0         | <u>19.7</u> | <b>8.3</b>  | <b>18.7</b> | <u>5.2</u> | <u>13.0</u> | <b>8.8</b> | <u>20.0</u> |

beam search, we adopt a beam width of 3 while maintaining the same temperature setting.

**Baselines.** We compare SAVER with two baseline decoding strategies (greedy decoding and beam search) as well as three SOTA hallucination mitigation methods, detailed as follows: Dola (Chuang et al. 2023) is specifically designed for alleviating hallucinations in factual tasks for LLMs by reducing shallow semantic influences to improve the factuality of the final layer’s output. OPERA (Huang et al. 2024) dynamically penalizes overconfident tokens based on the emergence of aggregation patterns, while proposing a retrospective allocation strategy to avoid cases where hallucinations have already occurred. Deco (Wang et al. 2024a) adaptively chooses relevant layers and integrates their knowledge into the final layer to adjust outputs. AGLA (An et al. 2024) uses an ensemble of global features for response generation and local features to mitigate hallucination. For all baseline methods, we use their official implementations and follow the recommended hyperparameter settings from the released source code to ensure fair comparisons.

**Benchmark and Metrics.** We evaluate the effectiveness, generalizability, and captioning quality of our method across five challenging benchmarks in both stylized and real-world scenarios: • **CHAIR.** Using the prompt “*Please describe the image in detail*,” we assess hallucination rates with CHAIRi and CHAIRs on our constructed dataset. Additionally, we evaluate captioning quality using BLEU-1/2/3/4 (Papineni et al. 2002), METEOR (Banerjee and Lavie 2005), and ROUGE-L (Lin 2004) which can be found in Appendix.

Table 3: Results on Style-POPE hallucination. “M.”, “L.” and “I.” stand for MiniGPT-4, LLaVA-1.5, and InstructBLIP.

| Method | Adversarial |             |             | Popular     |             |             | Random      |             |             | Overall Avg |             |             |
|--------|-------------|-------------|-------------|-------------|-------------|-------------|-------------|-------------|-------------|-------------|-------------|-------------|
|        | M.          | L.          | I.          | M.          | L.          | I.          | M.          | L.          | I.          | M.          | L.          | Ins.        |
| Dola   | 26.1        | 63.9        | 62.9        | 26.4        | 64.3        | 63.2        | 25.8        | 64.2        | 64.8        | 26.1        | 64.1        | 63.7        |
| Deco   | <b>67.0</b> | 73.3        | <b>73.6</b> | 66.8        | 74.6        | 72.2        | 70.8        | 80.5        | 82.7        | 68.2        | 76.2        | 76.2        |
| Ours   | <b>67.6</b> | <b>75.3</b> | <u>73.5</u> | <b>67.4</b> | <b>77.6</b> | <b>72.7</b> | <b>73.6</b> | <b>84.4</b> | <b>84.2</b> | <b>69.5</b> | <b>79.1</b> | <b>76.8</b> |

• **POPE.** Following the official POPE protocol, we report F1 scores as the primary metric. In the Appendix, we further incorporate ACC, Precision, and Recall to comprehensively evaluate our method. • **MME** (Fu et al. 2024) is a practical benchmark encompassing 14 sub-tasks, including OCR, visual knowledge, object recognition, and relational reasoning. • **Real-World Cases.** To evaluate performance beyond stylized images, we construct a dataset containing depth, thermal, medical, and RGB images with carefully designed query prompts. Additional details are available in the Appendix. • **AMBER.** (Wang et al. 2023a) To evaluate hallucination in more dimensions such as attribute, relation, and existence, we conduct experiments on the AMBER benchmark. More details are provided in the Appendix.

## Experimental Results

**Experiments on Style-CHAIR.** As shown in Tab. 2, our method consistently reduces hallucinations across all styles,

Table 4: Results on MME recognition related to the sub-tasks of commonsense reasoning, numerical calculation, text translation, and code reasoning.

| Model        | Method | Scene        | Num.        | Text.        | Code.       | Total Score  |
|--------------|--------|--------------|-------------|--------------|-------------|--------------|
| LLaVA-1.5    | Dola   | 58.6         | 60.0        | 82.5         | <b>57.5</b> | 258.6        |
|              | Deco   | 85.7         | 70.0        | 50.0         | 47.5        | 253.2        |
|              | Ours   | <b>88.6</b>  | <b>77.5</b> | <b>115.0</b> | 45.0        | <b>326.1</b> |
| InstructBLIP | Dola   | 81.4         | <b>55.0</b> | 57.5         | 45.0        | 238.9        |
|              | Deco   | 81.4         | 45.0        | <b>65.0</b>  | <b>72.5</b> | 263.9        |
|              | Ours   | <b>107.1</b> | 50.0        | 57.5         | 55.0        | <b>269.6</b> |

Table 5: Average Results on Real-World Benchmarks.

| Method | LLaVA-1.5   |             | MiniGPT-4   |             | InstructBLIP |             |
|--------|-------------|-------------|-------------|-------------|--------------|-------------|
|        | ACC         | F1          | ACC         | F1          | ACC          | F1          |
| Dola   | 62.2        | 62.4        | <b>55.4</b> | 37.2        | <b>65.8</b>  | 43.8        |
| Deco   | 57.4        | 69.4        | 50.2        | <b>66.4</b> | 60.0         | <b>68.2</b> |
| Ours   | <b>64.0</b> | <b>71.8</b> | 51.4        | <b>66.4</b> | 65.0         | <b>68.6</b> |

achieving the lowest average CHAIR across all evaluated models. Notably, SAVER achieves the best overall performance on MiniGPT-4 and InstructBLIP, clearly outperforming the SOTA method Deco. On LLaVA-1.5, SAVER achieves competitive results, closely matching the best scores. These results demonstrate the effectiveness of SAVER in mitigating object hallucinations for stylized images across diverse models and styles. Since captioning quality is critical for real-world applications, we further report the performance of different mitigation methods in terms of captioning quality in Tabs. 8, 9, and 10 in the Appendix. Compared to existing baselines, SAVER consistently exhibits outstanding text captioning performance.

**Experiments on Style-POPE and MME Benchmarks.** As shown in Tab. 3, SAVER consistently outperforms prior methods under various configurations on the Style-POPE benchmark, demonstrating superior robustness in mitigating hallucinations across adversarial, popular, and random settings. The detailed results are shown in Tab. 11, Tab. 12, and Tab. 13 in the Appendix. Additionally, in Tab. 4 and Tab. 14 (Appendix), SAVER achieves the highest scores across both perception and recognition tasks on the challenging MME benchmark, significantly improving performance for LLaVA-1.5 and InstructBLIP. Beyond stylized image captioning, SAVER exhibits strong generalizability to mitigate hallucinations in various practical challenging tasks.

**Experiments on Real-World Benchmarks.** To further examine SAVER’s practicability, we evaluate it on real-world scenarios, including depth, thermal, and medical images. As the average results shown in Tab. 5, SAVER consistently achieves the highest performance in different modalities. Specifically, it obtains the best average F1 scores of 71.8% on LLaVA-1.5 and 68.6% on InstructBLIP. These results further validate the effectiveness of SAVER in real-world

Table 6: Results on AMBER existence, attribute, and relation hallucination tasks with LLaVA-1.5-7b.

| Method | Existence   |             | Attribute   |             | Relation    |             |
|--------|-------------|-------------|-------------|-------------|-------------|-------------|
|        | Acc         | F1          | Acc         | F1          | Acc         | F1          |
| Dola   | 66.0        | <b>79.5</b> | 48.1        | 44.7        | 22.1        | 25.2        |
| Deco   | 63.1        | 62.5        | <b>67.2</b> | <b>53.5</b> | <b>69.5</b> | <b>48.1</b> |
| Ours   | <b>67.7</b> | <b>80.7</b> | <b>68.3</b> | <b>58.2</b> | <b>69.1</b> | <b>62.5</b> |

scenarios. The detailed results and discussions can be found in the Appendix.

**Experiments on AMBER Benchmarks.** Previous experiments comprehensively demonstrated SAVER’s effectiveness in mitigating object hallucination. Herein, we further evaluate SAVER’s generalizability on the AMBER dataset, which consists of three types of hallucinations, including existence, attribute, and relation. AMBER comprises 1,004 images, each paired with the corresponding designed questions and annotated labels. As shown in Tab. 6, SAVER consistently achieves the best or second-best Acc/F1 scores compared to the SOTA methods, exhibiting its strong generalizability to various hallucination types. This can be attributed to our visual early revision design that drives the model to pay more attention to visual signals.

### Ablation Study

Tabs. 16, 17, 18 and Fig. 6 in the Appendix detail the ablation experimental results. We vary five components—scale factor  $\alpha$ , confidence threshold  $p$ , candidate set size  $k$ , number of image-representative tokens  $N_i$ , and early-exit depth—to quantify their contributions to hallucination mitigation and caption fluency. For scale factor,  $\alpha = 0.6$  consistently balances visual grounding and language quality, attaining the lowest hallucination scores on LLaVA-1.5. For token filtering, higher thresholds reduce low confidence tokens. And  $p = 0.9$  achieves the strongest average results for MiniGPT-4 and InstructBLIP, while lower  $p$  preserves diversity in challenging styles at the cost of stability. In the candidate size,  $k = 20$  emerges as a robust optimum across models, and larger  $k$  introduces spurious evidence. Visual awareness is best supported by moderate  $N_i$  (50–100), as larger values can introduce low-confidence tokens that increase hallucination risks. Finally, the choice of early exit depth can greatly affect hallucinations. Experiments show that “Standard” provides the most stable performance.

### Conclusion

This work studies the high hallucination risk of existing LVLMs when understanding stylized images and how to mitigate it. By constructing a stylized dataset and a comprehensive benchmark, we demonstrate that stylized inputs significantly increase hallucination rates. To explore the underlying causes, we analyze the correlation between generated tokens and image tokens, revealing that the later layers of LVLMs tend to suppress visual information and rely more heavily on language priors. To address this, we propose

a training-free mitigation method, SAVER, which dynamically corrects generated tokens by retrieving optimal early layers with dense visual correlation. Extensive experiments across diverse models, datasets, and tasks validate the effectiveness of SAVER. We hope this work contributes to the development of more trustworthy LVLMs and facilitates their application in challenging scenarios.

## References

Abdin, M.; Jacobs, S. A.; Awan, A. A.; Aneja, J.; Awadallah, A.; Awadalla, H.; Bach, N.; Bahree, A.; Bakhtiari, A.; Behl, H.; et al. 2024. Phi-3 technical report: A highly capable language model locally on your phone. *arXiv preprint arXiv:2404.14219*.

AI, G. 2024. Gemini: A Large Language Model.

Alayrac, J.-B.; Donahue, J.; Luc, P.; Miech, A.; Barr, I.; Hasson, Y.; Lenc, K.; Mensch, A.; Millican, K.; Reynolds, M.; et al. 2022. Flamingo: a visual language model for few-shot learning. *Advances in neural information processing systems*, 35: 23716–23736.

An, W.; Tian, F.; Leng, S.; Nie, J.; Lin, H.; Wang, Q.; Dai, G.; Chen, P.; and Lu, S. 2024. Agla: Mitigating object hallucinations in large vision-language models with assembly of global and local attention. *arXiv preprint arXiv:2406.12718*.

Awadalla, A.; Gao, J.; Gardner, J.; Hessel, J.; Hanafy, Y.; Zhu, W.; Marathe, K.; Bitton, Y.; Gadre, S.; Sagawa, S.; et al. 2023. Openflamingo: An open-source framework for training large autoregressive vision-language models. *arXiv preprint arXiv:2308.01390*.

Bai, J.; Bai, S.; Yang, S.; Wang, S.; Tan, S.; Wang, P.; Lin, J.; Zhou, C.; and Zhou, J. 2023. Qwen-VL: A Versatile Vision-Language Model for Understanding, Localization, Text Reading, and Beyond. *arXiv preprint arXiv:2308.12966*.

Banerjee, S.; and Lavie, A. 2005. METEOR: An automatic metric for MT evaluation with improved correlation with human judgments. In *Proceedings of the acl workshop on intrinsic and extrinsic evaluation measures for machine translation and/or summarization*, 65–72.

Bavishi, R.; Elsen, E.; Hawthorne, C.; Nye, M.; Odena, A.; Soman, A.; and Taşırlar, S. 2023. Introducing our Multimodal Models.

Brie, P.; Burny, N.; Sluyters, A.; and Vanderdonckt, J. 2023. Evaluating a large language model on searching for gui layouts. *Proceedings of the ACM on Human-Computer Interaction*, 7(EICS): 1–37.

Cai, R.; Song, Z.; Guan, D.; Chen, Z.; Li, Y.; Luo, X.; Yi, C.; and Kot, A. 2024. Benchlmm: Benchmarking cross-style visual capability of large multimodal models. In *European Conference on Computer Vision*, 340–358. Springer.

Chen, J.; Zhang, T.; Huang, S.; Niu, Y.; Zhang, L.; Wen, L.; and Hu, X. 2024a. ICT: Image-Object Cross-Level Trusted Intervention for Mitigating Object Hallucination in Large Vision-Language Models. *arXiv preprint arXiv:2411.15268*.

Chen, K.; Zhang, Z.; Zeng, W.; Zhang, R.; Zhu, F.; and Zhao, R. 2023. Shikra: Unleashing multimodal llm’s referential dialogue magic. *arXiv preprint arXiv:2306.15195*.

Chen, L.; Sinavski, O.; Hünermann, J.; Karnsund, A.; Willmott, A. J.; Birch, D.; Maund, D.; and Shotton, J. 2024b. Driving with llms: Fusing object-level vector modality for explainable autonomous driving. In *2024 IEEE International Conference on Robotics and Automation (ICRA)*, 14093–14100. IEEE.

Chen, Z.; Wu, J.; Wang, W.; Su, W.; Chen, G.; Xing, S.; Zhong, M.; Zhang, Q.; Zhu, X.; Lu, L.; et al. 2024c. Internvl: Scaling up vision foundation models and aligning for generic visual-linguistic tasks. In *Proceedings of the IEEE/CVF Conference on Computer Vision and Pattern Recognition*, 24185–24198.

Chen, Z.; Zhao, Z.; Luo, H.; Yao, H.; Li, B.; and Zhou, J. 2024d. Halc: Object hallucination reduction via adaptive focal-contrast decoding. *arXiv preprint arXiv:2403.00425*.

Chiang, W.-L.; and Li, Z. 2 May 2025. Vicuna: An open-source chatbot impressing gpt-4 with 90%\* chatgpt quality.

Chuang, Y.-S.; Xie, Y.; Luo, H.; Kim, Y.; Glass, J.; and He, P. 2023. Dola: Decoding by contrasting layers improves factuality in large language models. *arXiv preprint arXiv:2309.03883*.

Dai, W.; Li, J.; Li, D.; Tiong, A. M. H.; Zhao, J.; Wang, W.; Li, B.; Fung, P.; and Hoi, S. 2023. InstructBLIP: Towards General-purpose Vision-Language Models with Instruction Tuning. *arXiv:2305.06500*.

Fu, C.; Chen, P.; Shen, Y.; Qin, Y.; Zhang, M.; Lin, X.; Yang, J.; Zheng, X.; Li, K.; Sun, X.; Wu, Y.; and Ji, R. 2024. MME: A Comprehensive Evaluation Benchmark for Multi-modal Large Language Models. *arXiv:2306.13394*.

Guan, T.; Liu, F.; Wu, X.; Xian, R.; Li, Z.; Liu, X.; Wang, X.; Chen, L.; Huang, F.; Yacoob, Y.; et al. 2024. Hallusion-bench: an advanced diagnostic suite for entangled language hallucination and visual illusion in large vision-language models. In *Proceedings of the IEEE/CVF Conference on Computer Vision and Pattern Recognition*, 14375–14385.

Hu, M.; Pan, S.; Li, Y.; and Yang, X. 2023. Advancing medical imaging with language models: A journey from n-grams to chatgpt. *arXiv preprint arXiv:2304.04920*.

Huang, Q.; Dong, X.; Zhang, P.; Wang, B.; He, C.; Wang, J.; Lin, D.; Zhang, W.; and Yu, N. 2024. Opera: Alleviating hallucination in multi-modal large language models via over-trust penalty and retrospection-allocation. In *Proceedings of the IEEE/CVF Conference on Computer Vision and Pattern Recognition*, 13418–13427.

Hwang, S.; Park, J.; Kim, N.; Choi, Y.; and Kweon, I. S. 2015. Multispectral Pedestrian Detection: Benchmark Dataset and Baselines. In *Proceedings of IEEE Conference on Computer Vision and Pattern Recognition (CVPR)*.

Jiang, Z.; Chen, J.; Zhu, B.; Luo, T.; Shen, Y.; and Yang, X. 2024. Devils in middle layers of large vision-language models: Interpreting, detecting and mitigating object hallucinations via attention lens. *arXiv preprint arXiv:2411.16724*.

Jing, L.; and Du, X. 2024. Fgaif: Aligning large vision-language models with fine-grained ai feedback. *arXiv preprint arXiv:2404.05046*.

Jing, L.; Li, R.; Chen, Y.; and Du, X. 2023. Faithscore: Fine-grained evaluations of hallucinations in large vision-language models. *arXiv preprint arXiv:2311.01477*.

Laurençon, H.; Tronchon, L.; Cord, M.; and Sanh, V. 2024. What matters when building vision-language models? *Advances in Neural Information Processing Systems*, 37: 87874–87907.

Leng, S.; Zhang, H.; Chen, G.; Li, X.; Lu, S.; Miao, C.; and Bing, L. 2024. Mitigating object hallucinations in large vision-language models through visual contrastive decoding. In *Proceedings of the IEEE/CVF Conference on Computer Vision and Pattern Recognition*, 13872–13882.

Li, J.; Li, D.; Savarese, S.; and Hoi, S. 2023a. Blip-2: Bootstrapping language-image pre-training with frozen image encoders and large language models. In *International conference on machine learning*, 19730–19742. PMLR.

Li, J.; Li, D.; Xiong, C.; and Hoi, S. 2022. Blip: Bootstrapping language-image pre-training for unified vision-language understanding and generation. In *International conference on machine learning*, 12888–12900. PMLR.

Li, Y.; Du, Y.; Zhou, K.; Wang, J.; Zhao, W. X.; and Wen, J.-R. 2023b. Evaluating object hallucination in large vision-language models. *arXiv preprint arXiv:2305.10355*.

Lin, C.-Y. 2004. Rouge: A package for automatic evaluation of summaries. In *Text summarization branches out*, 74–81.

Liu, H.; Li, C.; Li, Y.; and Lee, Y. J. 2024a. Improved baselines with visual instruction tuning. In *Proceedings of the IEEE/CVF Conference on Computer Vision and Pattern Recognition*, 26296–26306.

Liu, H.; Li, C.; Wu, Q.; and Lee, Y. J. 2023a. Visual instruction tuning. *Advances in neural information processing systems*, 36: 34892–34916.

Liu, H.; Li, C.; Wu, Q.; and Lee, Y. J. 2024b. Visual instruction tuning. *Advances in neural information processing systems*, 36.

Liu, H.; Zhu, Y.; Kato, K.; Kondo, I.; Aoyama, T.; and Hasegawa, Y. 2023b. Llm-based human-robot collaboration framework for manipulation tasks. *arXiv preprint arXiv:2308.14972*.

OpenAI. 2023. GPT-4 Technical Report. <https://openai.com/research/gpt-4>. Accessed: 2024-10-18.

Papineni, K.; Roukos, S.; Ward, T.; and Zhu, W.-J. 2002. Bleu: a method for automatic evaluation of machine translation. In *Proceedings of the 40th annual meeting of the Association for Computational Linguistics*, 311–318.

Rohrbach, A.; Hendricks, L. A.; Burns, K.; Darrell, T.; and Saenko, K. 2018. Object hallucination in image captioning. *arXiv preprint arXiv:1809.02156*.

Silberman, N.; Hoiem, D.; Kohli, P.; and Fergus, R. 2012. Indoor segmentation and support inference from rgbd images. In *Computer Vision–ECCV 2012: 12th European Conference on Computer Vision, Florence, Italy, October 7–13, 2012, Proceedings, Part V 12*, 746–760. Springer.

Sun, Z.; Shen, S.; Cao, S.; Liu, H.; Li, C.; Shen, Y.; Gan, C.; Gui, L.-Y.; Wang, Y.-X.; Yang, Y.; et al. 2023. Aligning large multimodal models with factually augmented rlhf. *arXiv preprint arXiv:2309.14525*.

Suo, W.; Zhang, L.; Sun, M.; Wu, L. Y.; Wang, P.; and Zhang, Y. 2025. Octopus: Alleviating Hallucination via Dynamic Contrastive Decoding. *arXiv preprint arXiv:2503.00361*.

Touvron, H.; Lavril, T.; Izacard, G.; Martinet, X.; Lachaux, M.-A.; Lacroix, T.; Rozière, B.; Goyal, N.; Hambro, E.; Azhar, F.; et al. 2023. Llama: Open and efficient foundation language models. *arXiv preprint arXiv:2302.13971*.

Wang, C.; Chen, X.; Zhang, N.; Tian, B.; Xu, H.; Deng, S.; and Chen, H. 2024a. Mllm can see? dynamic correction decoding for hallucination mitigation. *arXiv preprint arXiv:2410.11779*.

Wang, H.; Wang, Q.; Bai, X.; Qin, Z.; and Chen, A. 2024b. InstantStyle: Free Lunch towards Style-Preserving in Text-to-Image Generation. *arXiv preprint arXiv:2404.02733*.

Wang, J.; Wang, Y.; Xu, G.; Zhang, J.; Gu, Y.; Jia, H.; Wang, J.; Xu, H.; Yan, M.; Zhang, J.; et al. 2023a. Amber: An llm-free multi-dimensional benchmark for mllms hallucination evaluation. *arXiv preprint arXiv:2311.07397*.

Wang, L.; He, J.; Li, S.; Liu, N.; and Lim, E.-P. 2024c. Mitigating fine-grained hallucination by fine-tuning large vision-language models with caption rewrites. In *International Conference on Multimedia Modeling*, 32–45. Springer.

Wang, S.; Zhao, Z.; Ouyang, X.; Wang, Q.; and Shen, D. 2023b. Chatcad: Interactive computer-aided diagnosis on medical image using large language models. *arXiv preprint arXiv:2302.07257*.

Xie, Y.; Li, G.; Xu, X.; and Kan, M.-Y. 2024. V-dpo: Mitigating hallucination in large vision language models via vision-guided direct preference optimization. *arXiv preprint arXiv:2411.02712*.

Xing, Y.; Li, Y.; Laptev, I.; and Lu, S. 2024. Mitigating object hallucination via concentric causal attention. *Advances in Neural Information Processing Systems*, 37: 92012–92035.

Yang, L.; Zheng, Z.; Chen, B.; Zhao, Z.; Lin, C.; and Shen, C. 2024. Nullu: Mitigating Object Hallucinations in Large Vision-Language Models via HalluSpace Projection. *arXiv preprint arXiv:2412.13817*.

Ye, Q.; Xu, H.; Ye, J.; Yan, M.; Hu, A.; Liu, H.; Qian, Q.; Zhang, J.; and Huang, F. 2024. mplug-owl2: Revolutionizing multi-modal large language model with modality collaboration. In *Proceedings of the ieee/cvf conference on computer vision and pattern recognition*, 13040–13051.

Yin, S.; Fu, C.; Zhao, S.; Li, K.; Sun, X.; Xu, T.; and Chen, E. 2024a. A survey on multimodal large language models. *National Science Review*, 11(12).

Yin, S.; Fu, C.; Zhao, S.; Xu, T.; Wang, H.; Sui, D.; Shen, Y.; Li, K.; Sun, X.; and Chen, E. 2024b. Woodpecker: Hallucination correction for multimodal large language models. *Science China Information Sciences*, 67(12): 220105.

Yu, T.; Zhang, H.; Li, Q.; Xu, Q.; Yao, Y.; Chen, D.; Lu, X.; Cui, G.; Dang, Y.; He, T.; et al. 2025. Rlaif-v: Open-source ai feedback leads to super gpt-4v trustworthiness. In *Proceedings of the Computer Vision and Pattern Recognition Conference*, 19985–19995.

Yue, Z.; Zhang, L.; and Jin, Q. 2024. Less is more: Mitigating multimodal hallucination from an eos decision perspective. *arXiv preprint arXiv:2402.14545*.

Zhang, J.; Wang, T.; Zhang, H.; Lu, P.; and Zheng, F. 2024a. Reflective instruction tuning: Mitigating hallucinations in large vision-language models. In *European Conference on Computer Vision*, 196–213. Springer.

Zhang, Y.-K.; Lu, S.; Li, Y.; Ma, Y.; Chen, Q.; Xu, Z.; Luo, W.; Zhang, K.; Zhan, D.-C.; and Ye, H.-J. 2024b. Wings: Learning multimodal llms without text-only forgetting. *Advances in Neural Information Processing Systems*, 37: 31828–31853.

Zhao, Z.; Tang, J.; Wu, B.; Lin, C.; Wei, S.; Liu, H.; Tan, X.; Zhang, Z.; Huang, C.; and Xie, Y. 2024. Harmonizing visual text comprehension and generation. *arXiv preprint arXiv:2407.16364*.

Zhou, B.; Hu, Y.; Weng, X.; Jia, J.; Luo, J.; Liu, X.; Wu, J.; and Huang, L. 2024. TinyLLaVA: A Framework of Small-scale Large Multimodal Models. *arXiv:2402.14289*.

Zhou, Y.; Cui, C.; Yoon, J.; Zhang, L.; Deng, Z.; Finn, C.; Bansal, M.; and Yao, H. 2023. Analyzing and mitigating object hallucination in large vision-language models. *arXiv preprint arXiv:2310.00754*.

Zhu, D.; Chen, J.; Shen, X.; Li, X.; and Elhoseiny, M. 2023. Minigpt-4: Enhancing vision-language understanding with advanced large language models. *arXiv preprint arXiv:2304.10592*.

Zhuang, X.; Zhu, Z.; Chen, Z.; Xie, Y.; Liang, L.; and Zou, Y. 2024. Game on Tree: Visual Hallucination Mitigation via Coarse-to-Fine View Tree and Game Theory. In *Proceedings of the 2024 Conference on Empirical Methods in Natural Language Processing*, 17984–18003.

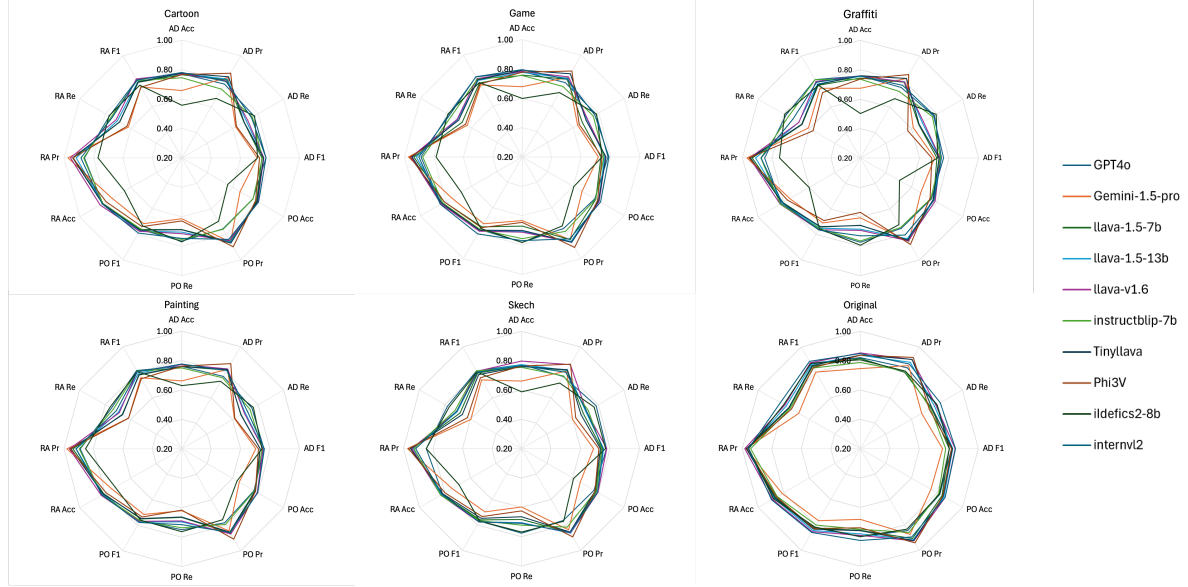


Figure 5: Style-POPE benchmark results.

Table 7: Style-Chair benchmark with prompt: “*Provide a one-sentence caption for the provided image.*” Lower Ci and Cs indicate fewer hallucinations.

| Model                 | Cartoon |      |      |      | Game |      |      |      | Graffiti |      |      |      | Painting |      |    |    | Sketch |    |    |    | Original |    |    |    | Average |  |
|-----------------------|---------|------|------|------|------|------|------|------|----------|------|------|------|----------|------|----|----|--------|----|----|----|----------|----|----|----|---------|--|
|                       | Ci      | Cs   | Ci   | Cs   | Ci   | Cs   | Ci   | Cs   | Ci       | Cs   | Ci   | Cs   | Ci       | Cs   | Ci | Cs | Ci     | Cs | Ci | Cs | Ci       | Cs | Ci | Cs |         |  |
| GPT4o                 | 6.2     | 7.0  | 3.1  | 3.7  | 2.4  | 2.7  | 4.3  | 6.0  | 3.6      | 5.0  | 0.7  | 0.5  | 3.4      | 4.2  |    |    |        |    |    |    |          |    |    |    |         |  |
| Gemini-1.5-PRO        | 4.9     | 6.0  | 3.0  | 4.3  | 2.3  | 2.7  | 6.9  | 9.0  | 3.4      | 4.7  | 2.3  | 3.7  | 3.8      | 5.1  |    |    |        |    |    |    |          |    |    |    |         |  |
| LLaVA-1.5             | 9.1     | 19.3 | 7.2  | 14.0 | 8.2  | 16.0 | 6.9  | 13.0 | 7.1      | 13.7 | 2.6  | 5.7  | 6.9      | 13.6 |    |    |        |    |    |    |          |    |    |    |         |  |
| LLaVA-1.5-13b         | 8.1     | 16.7 | 5.4  | 10.3 | 8.9  | 17.3 | 6.6  | 13.3 | 6.2      | 12.3 | 4.3  | 8.7  | 6.6      | 13.1 |    |    |        |    |    |    |          |    |    |    |         |  |
| LLaVA-v1.6-mistral-7b | 6.5     | 8.7  | 3.2  | 4.3  | 4.1  | 5.3  | 4.8  | 6.7  | 4.4      | 6.0  | 1.2  | 1.7  | 4.0      | 5.5  |    |    |        |    |    |    |          |    |    |    |         |  |
| InstructBLIP          | 5.8     | 10.3 | 5.0  | 9.0  | 5.2  | 8.3  | 3.0  | 5.0  | 4.3      | 6.7  | 2.0  | 4.0  | 4.2      | 7.2  |    |    |        |    |    |    |          |    |    |    |         |  |
| MiniGPT-4-7b          | 11.4    | 27.0 | 9.1  | 20.3 | 10.5 | 21.0 | 9.0  | 21.7 | 9.4      | 23.3 | 5.4  | 14.0 | 9.1      | 21.2 |    |    |        |    |    |    |          |    |    |    |         |  |
| Tinyllava             | 6.1     | 12.3 | 5.6  | 11.7 | 5.8  | 12.3 | 5.2  | 11.3 | 6.6      | 14.0 | 2.5  | 5.3  | 5.3      | 11.2 |    |    |        |    |    |    |          |    |    |    |         |  |
| Phi3V                 | 7.9     | 14.0 | 5.9  | 11.0 | 8.0  | 13.7 | 6.8  | 11.7 | 6.3      | 12.0 | 3.1  | 5.3  | 6.3      | 11.3 |    |    |        |    |    |    |          |    |    |    |         |  |
| Fuyu                  | 20.6    | 69.3 | 19.1 | 69.7 | 25.0 | 59.3 | 16.9 | 58.7 | 19.7     | 53.7 | 14.9 | 59.3 | 19.4     | 61.7 |    |    |        |    |    |    |          |    |    |    |         |  |
| Idefics2-8b           | 9.7     | 14.0 | 6.8  | 9.7  | 6.6  | 9.7  | 5.8  | 9.7  | 6.0      | 9.0  | 2.7  | 5.0  | 6.3      | 9.5  |    |    |        |    |    |    |          |    |    |    |         |  |
| mPLUG-Owl2            | 5.6     | 8.3  | 5.6  | 8.3  | 6.2  | 8.0  | 4.7  | 6.0  | 4.3      | 6.3  | 1.6  | 2.7  | 4.7      | 6.6  |    |    |        |    |    |    |          |    |    |    |         |  |
| Qwen-VL               | 8.4     | 15.0 | 6.4  | 13.0 | 9.5  | 14.7 | 7.1  | 12.0 | 7.4      | 14.3 | 3.1  | 6.3  | 7.0      | 12.6 |    |    |        |    |    |    |          |    |    |    |         |  |

## Appendix

### Style-POPE Benchmark

Here we present the Style-POPE hallucination benchmark results on existing LVLMs as shown in Fig. 5, including GPT-4o (OpenAI 2023), Gemini-1.5-Pro (AI 2024), three variants of LLaVA (LLaVA-1.5-7B, LLaVA-1.5-13B, and LLaVA-1.6) (Liu et al. 2024b), InstructBLIP-7B (Dai et al. 2023), TinyLLaVA (Zhou et al. 2024), Phi3V (Abdin et al. 2024), IDEFICS2-8B (Laurençon et al. 2024), and InternVL2 (Chen et al. 2024c). We report accuracy, precision, recall, and F1 scores across Adversarial, Popular, and Random settings to comprehensively benchmark the LVLMs’ hallucination performance in various styles. It can be observed that GPT-4o and Gemini-1.5-Pro consistently achieve superior hallucination evaluation scores, demonstrating their outstanding visual understanding performance. In addition, the evaluation results on original photographs largely outperform the other five styles across all POPE metrics, proving that LVLMs tend to produce more hallucinations with style images, aligning with our findings discussed in the main manuscript.

### Style-Chair Benchmark

Here we present an extended analysis and results of our Chair benchmark using a different prompt. Tab. 7 summarizes hallucination rates on the Style-CHAIR benchmark using the prompt “*Provide a one-sentence caption for the provided image.*” Similarly, the benchmark results show existing LVLMs have higher CHAIR scores in five styles. Compared to Tab. 1, the benchmark results in Tab. 7 indicate that more detailed captions may produce more hallucinations, and LVLMs generate more hallucinations for style images.

## Evaluation on Captioning Quality

While SAVER is explicitly designed to reduce object hallucinations, maintaining captioning fluency and informativeness is also crucial for practical applications. Tabs. 8, 9, and 10 present standard n-gram-based metrics (BLEU-1–4, METEOR, and ROUGE-L) evaluated on the generated captions of three models: InstructBLIP, LLaVA-1.5, and MiniGPT-4. Overall, these results demonstrate that SAVER can significantly mitigate hallucination while negligibly affecting captioning quality.

Table 8: Captioning quality scores on InstructBLIP.

| Style    | Method | Bleu1 | Bleu2 | Bleu3 | Bleu4 | METEOR | ROUGE_L |
|----------|--------|-------|-------|-------|-------|--------|---------|
| Cartoon  | Greedy | 24.4  | 11.7  | 6.4   | 3.5   | 17.2   | 20.4    |
|          | Beam   | 27.2  | 16.5  | 10.1  | 6.2   | 20.0   | 26.4    |
|          | OPERA  | 27.7  | 17.3  | 10.7  | 6.7   | 20.4   | 26.7    |
|          | Deco   | 24.8  | 15.2  | 9.0   | 5.3   | 18.3   | 24.1    |
|          | AGLA   | 26.2  | 16.9  | 10.4  | 6.4   | 20.0   | 25.6    |
|          | Ours   | 25.1  | 15.9  | 9.7   | 6.0   | 19.4   | 24.6    |
| Game     | Greedy | 24.4  | 11.8  | 6.6   | 3.6   | 17.4   | 20.4    |
|          | Beam   | 27.3  | 16.9  | 10.3  | 6.3   | 20.7   | 26.0    |
|          | OPERA  | 27.7  | 17.3  | 10.6  | 6.5   | 20.7   | 26.3    |
|          | Deco   | 25.0  | 15.8  | 9.6   | 5.8   | 19.0   | 24.6    |
|          | AGLA   | 26.7  | 17.4  | 10.8  | 6.7   | 20.6   | 26.0    |
|          | Ours   | 25.0  | 16.2  | 10.0  | 6.1   | 19.8   | 24.5    |
| Graffiti | Greedy | 24.2  | 11.0  | 5.6   | 2.8   | 16.6   | 20.7    |
|          | Beam   | 27.2  | 16.4  | 9.8   | 5.9   | 19.7   | 26.1    |
|          | OPERA  | 27.3  | 17.0  | 10.4  | 6.5   | 20.1   | 26.8    |
|          | Deco   | 24.2  | 14.9  | 8.6   | 5.0   | 18.0   | 23.8    |
|          | AGLA   | 26.4  | 17.0  | 10.3  | 6.2   | 19.5   | 25.8    |
|          | Ours   | 24.5  | 15.5  | 9.3   | 5.7   | 18.8   | 24.3    |
| Painting | Greedy | 24.2  | 11.2  | 6.0   | 3.2   | 17.0   | 20.0    |
|          | Beam   | 27.3  | 16.8  | 10.1  | 6.1   | 20.5   | 25.7    |
|          | OPERA  | 27.5  | 17.1  | 10.3  | 6.2   | 20.5   | 26.0    |
|          | Deco   | 24.2  | 15.0  | 8.8   | 5.2   | 18.5   | 24.0    |
|          | AGLA   | 26.1  | 16.7  | 10.3  | 6.5   | 20.2   | 25.6    |
|          | Ours   | 24.6  | 15.7  | 9.3   | 5.5   | 19.3   | 24.1    |
| Sketch   | Greedy | 24.0  | 11.3  | 6.1   | 3.4   | 16.9   | 19.8    |
|          | Beam   | 26.9  | 16.7  | 10.2  | 6.4   | 20.4   | 25.5    |
|          | OPERA  | 27.4  | 17.5  | 10.8  | 6.8   | 20.6   | 26.2    |
|          | Deco   | 24.6  | 15.3  | 9.0   | 5.3   | 18.7   | 23.9    |
|          | AGLA   | 26.4  | 17.2  | 10.5  | 6.4   | 20.3   | 25.2    |
|          | Ours   | 25.0  | 16.1  | 9.8   | 6.0   | 19.7   | 24.6    |
| Original | Greedy | 27.9  | 14.5  | 8.3   | 4.8   | 20.3   | 22.8    |
|          | Beam   | 30.9  | 20.1  | 12.8  | 8.3   | 23.8   | 28.7    |
|          | OPERA  | 31.5  | 21.0  | 13.6  | 8.8   | 24.1   | 29.5    |
|          | Deco   | 28.3  | 18.8  | 11.9  | 7.5   | 22.2   | 27.2    |
|          | AGLA   | 30.1  | 20.3  | 13.2  | 8.5   | 23.5   | 28.9    |
|          | Ours   | 29.5  | 20.3  | 13.1  | 8.4   | 23.6   | 28.2    |

Table 9: Captioning quality scores on LLaVA-1.5.

| Style    | Method | Bleu1 | Bleu2 | Bleu3 | Bleu4 | METEOR | ROUGE_L |
|----------|--------|-------|-------|-------|-------|--------|---------|
| Cartoon  | Greedy | 25.9  | 16.4  | 9.9   | 6.1   | 19.9   | 25.5    |
|          | Beam   | 26.9  | 16.4  | 9.8   | 5.9   | 20.2   | 26.0    |
|          | OPERA  | 26.9  | 16.7  | 10.1  | 6.2   | 20.2   | 26.1    |
|          | Deco   | 25.5  | 15.3  | 9.0   | 5.4   | 18.7   | 24.4    |
|          | AGLA   | 26.2  | 16.1  | 9.6   | 5.8   | 19.7   | 25.4    |
|          | Ours   | 25.3  | 14.8  | 8.4   | 4.9   | 18.5   | 24.0    |
| Game     | Greedy | 26.8  | 17.2  | 10.5  | 6.4   | 20.3   | 25.7    |
|          | Beam   | 26.9  | 16.7  | 10.1  | 6.1   | 20.4   | 25.8    |
|          | OPERA  | 27.1  | 17.0  | 10.2  | 6.2   | 20.5   | 26.0    |
|          | Deco   | 25.7  | 15.5  | 9.1   | 5.4   | 19.1   | 24.6    |
|          | AGLA   | 26.5  | 16.8  | 10.1  | 6.2   | 20.3   | 25.5    |
|          | Ours   | 25.2  | 15.3  | 8.8   | 5.0   | 18.5   | 24.1    |
| Graffiti | Greedy | 26.0  | 16.7  | 10.4  | 6.6   | 20.0   | 25.3    |
|          | Beam   | 26.5  | 16.5  | 10.1  | 6.3   | 20.1   | 25.6    |
|          | OPERA  | 26.2  | 16.4  | 10.1  | 6.3   | 19.8   | 25.4    |
|          | Deco   | 25.0  | 15.0  | 8.8   | 5.2   | 18.3   | 24.0    |
|          | AGLA   | 25.8  | 16.3  | 9.9   | 6.1   | 19.7   | 25.0    |
|          | Ours   | 24.7  | 14.6  | 8.3   | 4.8   | 18.2   | 23.7    |
| Painting | Greedy | 26.6  | 17.0  | 10.3  | 6.2   | 20.3   | 25.8    |
|          | Beam   | 26.7  | 16.2  | 9.7   | 5.9   | 20.1   | 25.7    |
|          | OPERA  | 26.9  | 16.6  | 10.0  | 6.1   | 20.2   | 25.8    |
|          | Deco   | 25.0  | 14.9  | 8.4   | 4.8   | 18.5   | 24.0    |
|          | AGLA   | 26.5  | 16.4  | 9.7   | 5.7   | 20.2   | 25.5    |
|          | Ours   | 25.2  | 14.8  | 8.3   | 4.8   | 18.5   | 23.9    |
| Sketch   | Greedy | 25.7  | 16.5  | 10.1  | 6.1   | 20.1   | 24.7    |
|          | Beam   | 26.5  | 16.6  | 10.1  | 6.2   | 20.1   | 25.4    |
|          | OPERA  | 26.0  | 16.2  | 9.7   | 5.9   | 20.0   | 25.4    |
|          | Deco   | 25.3  | 15.2  | 8.8   | 5.1   | 18.8   | 24.1    |
|          | AGLA   | 25.9  | 16.4  | 9.9   | 5.9   | 19.8   | 24.8    |
|          | Ours   | 24.9  | 14.8  | 8.3   | 4.7   | 18.3   | 23.9    |
| Original | Greedy | 29.1  | 19.3  | 12.3  | 7.8   | 23.0   | 27.8    |
|          | Beam   | 30.1  | 19.8  | 12.6  | 8.1   | 23.5   | 28.6    |
|          | OPERA  | 30.1  | 19.8  | 12.7  | 8.2   | 23.3   | 28.5    |
|          | Deco   | 27.9  | 17.7  | 10.8  | 6.5   | 21.5   | 26.1    |
|          | AGLA   | 29.5  | 19.3  | 12.2  | 7.7   | 23.1   | 27.7    |
|          | Ours   | 27.3  | 17.1  | 10.4  | 6.3   | 20.9   | 25.8    |

Table 10: Captioning quality scores on MiniGPT-4.

| Style    | Method | Bleu1 | Bleu2 | Bleu3 | Bleu4 | METEOR | ROUGE_L |
|----------|--------|-------|-------|-------|-------|--------|---------|
| Cartoon  | Greedy | 25.8  | 16.6  | 10.3  | 6.5   | 19.6   | 25.1    |
|          | Beam   | 26.6  | 16.9  | 10.6  | 6.8   | 19.8   | 25.5    |
|          | OPERA  | 26.9  | 17.2  | 10.9  | 6.9   | 19.8   | 26.1    |
|          | Deco   | 25.3  | 15.6  | 9.3   | 5.4   | 18.6   | 23.9    |
|          | AGLA   | 19.5  | 12.8  | 8.0   | 5.0   | 17.6   | 20.9    |
|          | Ours   | 25.3  | 16.0  | 9.8   | 5.9   | 19.0   | 24.9    |
| Game     | Greedy | 26.2  | 17.2  | 10.9  | 7.0   | 20.1   | 25.1    |
|          | Beam   | 26.7  | 17.4  | 11.0  | 7.0   | 20.3   | 25.7    |
|          | OPERA  | 27.3  | 17.8  | 11.3  | 7.2   | 20.6   | 26.4    |
|          | Deco   | 25.9  | 16.3  | 9.9   | 6.0   | 19.0   | 24.6    |
|          | AGLA   | 19.2  | 12.6  | 7.8   | 4.9   | 17.5   | 20.7    |
|          | Ours   | 25.7  | 16.6  | 10.2  | 6.3   | 19.6   | 25.1    |
| Graffiti | Greedy | 25.5  | 16.5  | 10.4  | 6.6   | 19.6   | 25.0    |
|          | Beam   | 26.3  | 16.7  | 10.4  | 6.6   | 19.9   | 25.3    |
|          | OPERA  | 26.5  | 17.1  | 10.8  | 7.0   | 19.9   | 25.7    |
|          | Deco   | 25.2  | 15.7  | 9.5   | 5.9   | 18.5   | 24.5    |
|          | AGLA   | 20.4  | 13.4  | 8.3   | 5.2   | 17.9   | 21.6    |
|          | Ours   | 25.5  | 16.4  | 10.0  | 6.1   | 19.0   | 25.3    |
| Painting | Greedy | 26.3  | 17.3  | 10.9  | 7.0   | 20.3   | 25.6    |
|          | Beam   | 26.6  | 17.3  | 10.8  | 6.9   | 20.4   | 25.9    |
|          | OPERA  | 26.7  | 17.5  | 11.0  | 7.1   | 20.5   | 26.3    |
|          | Deco   | 25.5  | 16.0  | 9.8   | 5.9   | 19.4   | 24.3    |
|          | AGLA   | 19.9  | 13.1  | 8.1   | 5.0   | 17.8   | 20.8    |
|          | Ours   | 25.5  | 16.3  | 10.0  | 6.1   | 19.2   | 25.0    |
| Sketch   | Greedy | 26.6  | 17.5  | 11.1  | 7.1   | 20.4   | 25.4    |
|          | Beam   | 27.2  | 17.9  | 11.5  | 7.4   | 21.1   | 26.2    |
|          | OPERA  | 27.2  | 18.0  | 11.6  | 7.5   | 20.9   | 26.3    |
|          | Deco   | 25.9  | 16.2  | 10.0  | 6.1   | 19.4   | 24.4    |
|          | AGLA   | 20.3  | 13.4  | 8.3   | 5.1   | 18.1   | 21.2    |
|          | Ours   | 26.0  | 16.7  | 10.2  | 6.3   | 19.9   | 25.2    |
| Original | Greedy | 29.0  | 19.9  | 13.2  | 8.6   | 23.1   | 27.5    |
|          | Beam   | 29.8  | 20.3  | 13.4  | 8.7   | 23.2   | 28.1    |
|          | OPERA  | 30.2  | 20.9  | 13.9  | 9.0   | 23.7   | 28.8    |
|          | Deco   | 28.5  | 18.9  | 12.1  | 7.7   | 22.1   | 26.5    |
|          | AGLA   | 21.0  | 14.4  | 9.2   | 5.7   | 19.7   | 22.0    |
|          | Ours   | 29.0  | 20.2  | 13.3  | 8.6   | 23.0   | 28.0    |

## Detailed Hallucination Mitigation Results on Style-POPE

Tabs. 11, 12, and 13 report the results on the Style-POPE benchmark for MiniGPT-4 (Zhu et al. 2023), InstructBLIP (Dai et al. 2023), and LLaVA-1.5 (Liu et al. 2024b) across three evaluation settings: Adversarial, Popular, and Random. Our proposed method, SAVER, consistently achieves superior hallucination mitigation performance across various experimental settings, evaluation metrics, and models. Specifically, SAVER enhances accuracy across every style–sampling combination for MiniGPT-4, with the most substantial improvement observed in the Painting style under Random sampling, where accuracy rises significantly from 60.2% to 67.9%. Similarly, for LLaVA-1.5 under the Random sampling setting of Original images, SAVER boosts accuracy from 82.8% to 88.2%, alongside proportional increases in precision and F1 scores. Furthermore, SAVER can still achieve performance gains on InstructBLIP. These results highlight SAVER’s significant improvements across diverse LVLM architectures and sampling strategies, underscoring its effectiveness in mitigating object hallucinations for style images.

Table 11: Style-POPE benchmark results on MiniGPT-4.

| Style    | Method      | Adversarial  |           |        |              | Popular      |           |        |              | Random       |           |        |              |
|----------|-------------|--------------|-----------|--------|--------------|--------------|-----------|--------|--------------|--------------|-----------|--------|--------------|
|          |             | ACC          | Precision | Recall | F1           | ACC          | Precision | Recall | F1           | ACC          | Precision | Recall | F1           |
| Cartoon  | Dola        | 52.10        | 57.30     | 16.60  | 25.70        | <b>53.40</b> | 63.10     | 16.60  | 26.20        | 48.70        | 46.40     | 16.60  | 24.40        |
|          | Deco        | 51.30        | 50.70     | 98.10  | 66.80        | 50.90        | 50.50     | 98.10  | 66.60        | 56.60        | 53.60     | 98.10  | 69.30        |
|          | SAVER(Ours) | <b>53.80</b> | 52.10     | 94.20  | <b>67.10</b> | 53.10        | 51.70     | 94.20  | <b>66.70</b> | <b>63.90</b> | 58.60     | 94.20  | <b>72.30</b> |
| Game     | Dola        | 53.60        | 60.90     | 19.90  | 30.00        | 54.80        | 66.10     | 19.90  | 30.60        | 51.70        | 54.70     | 19.90  | 29.20        |
|          | Deco        | 51.40        | 50.80     | 97.60  | 66.80        | 51.00        | 50.50     | 97.60  | 66.60        | 58.00        | 54.50     | 97.60  | 69.90        |
|          | SAVER(Ours) | <b>54.60</b> | 52.60     | 93.80  | <b>67.40</b> | <b>54.20</b> | 52.30     | 93.80  | <b>67.20</b> | <b>64.40</b> | 59.10     | 93.80  | <b>72.50</b> |
| Graffiti | Dola        | 50.60        | 53.20     | 10.20  | 17.10        | 51.60        | 59.00     | 10.20  | 17.40        | 49.40        | 47.20     | 10.20  | 16.80        |
|          | Deco        | 51.70        | 50.90     | 97.60  | 66.90        | 50.90        | 50.50     | 97.60  | 66.50        | 56.80        | 53.70     | 97.60  | 69.30        |
|          | SAVER(Ours) | <b>54.20</b> | 52.40     | 93.70  | <b>67.20</b> | <b>53.60</b> | 52.00     | 93.70  | <b>66.90</b> | <b>63.40</b> | 58.30     | 93.70  | <b>71.90</b> |
| Painting | Dola        | 49.70        | 48.90     | 12.80  | 20.30        | 50.20        | 50.90     | 12.80  | 20.40        | 48.70        | 45.30     | 12.80  | 19.90        |
|          | Deco        | 51.80        | 51.00     | 97.90  | 67.00        | 51.90        | 51.00     | 97.90  | 67.10        | 60.20        | 55.80     | 97.90  | 71.10        |
|          | SAVER(Ours) | <b>55.40</b> | 53.10     | 92.80  | <b>67.50</b> | <b>54.70</b> | 52.60     | 92.80  | <b>67.20</b> | <b>67.90</b> | 61.90     | 92.80  | <b>74.30</b> |
| Sketch   | Dola        | 14.10        | 51.70     | 56.90  | 13.70        | 12.00        | 53.20     | 65.40  | 13.70        | 10.40        | 51.50     | 56.20  | 13.70        |
|          | Deco        | 52.20        | 51.20     | 98.10  | 67.30        | 51.90        | 51.00     | 98.10  | 67.10        | 58.90        | 55.00     | 98.10  | 70.50        |
|          | SAVER(Ours) | <b>55.40</b> | 53.10     | 93.10  | <b>67.60</b> | <b>55.40</b> | 53.10     | 93.10  | <b>67.60</b> | <b>65.30</b> | 59.90     | 93.10  | <b>72.90</b> |
| Original | Dola        | 54.20        | 55.20     | 45.10  | 49.60        | 55.00        | 56.20     | 45.10  | 50.10        | 55.90        | 57.50     | 45.10  | 50.60        |
|          | Deco        | 54.50        | 52.50     | 94.60  | 67.50        | 53.20        | 51.80     | 94.60  | 66.90        | 68.20        | 61.90     | 94.60  | 74.80        |
|          | SAVER(Ours) | <b>60.40</b> | 56.80     | 86.90  | <b>68.70</b> | <b>60.20</b> | 56.60     | 86.90  | <b>68.60</b> | <b>75.00</b> | 70.20     | 86.90  | <b>77.70</b> |
| Average  | Dola        | 45.72        | 54.53     | 26.92  | 26.07        | 46.17        | 58.08     | 28.33  | 26.40        | 44.13        | 50.43     | 26.80  | 25.77        |
|          | Deco        | 52.15        | 51.18     | 97.32  | 67.05        | 51.63        | 50.88     | 97.32  | 66.80        | 59.78        | 55.75     | 97.32  | 70.82        |
|          | SAVER(Ours) | <b>55.63</b> | 53.35     | 92.42  | <b>67.58</b> | <b>55.20</b> | 53.05     | 92.42  | <b>67.37</b> | <b>66.65</b> | 61.33     | 92.42  | <b>73.60</b> |

Table 12: Style-POPE benchmark results on InstructBLIP.

| Style    | Method      | Adversarial  |           |        |              | Popular      |           |        |              | Random       |           |        |              |
|----------|-------------|--------------|-----------|--------|--------------|--------------|-----------|--------|--------------|--------------|-----------|--------|--------------|
|          |             | ACC          | Precision | Recall | F1           | ACC          | Precision | Recall | F1           | ACC          | Precision | Recall | F1           |
| Cartoon  | Dola        | <b>70.90</b> | 87.80     | 48.70  | 62.60        | <b>71.30</b> | 89.00     | 48.70  | 62.90        | 73.80        | 98.00     | 48.70  | 65.00        |
|          | Deco        | 66.90        | 61.80     | 88.40  | 72.80        | 63.30        | 58.90     | 88.40  | 70.70        | 78.90        | 74.30     | 88.40  | 80.70        |
|          | SAVER(Ours) | 67.90        | 62.90     | 87.00  | <b>73.00</b> | 64.90        | 60.40     | 87.00  | <b>71.30</b> | <b>82.40</b> | 79.70     | 87.00  | <b>83.20</b> |
| Game     | Dola        | <b>72.60</b> | 90.80     | 50.30  | 64.80        | <b>72.90</b> | 91.90     | 50.30  | 65.00        | 74.70        | 98.10     | 50.30  | 66.50        |
|          | Deco        | 67.40        | 62.40     | 87.90  | 73.00        | 64.20        | 59.60     | 87.90  | 71.00        | 79.50        | 75.30     | 87.90  | 81.10        |
|          | SAVER(Ours) | 68.10        | 63.30     | 86.40  | <b>73.10</b> | 66.30        | 61.60     | 86.40  | <b>71.90</b> | <b>82.60</b> | 80.20     | 86.40  | <b>83.20</b> |
| Graffiti | Dola        | <b>69.90</b> | 90.20     | 44.80  | 59.80        | 70.20        | 91.20     | 44.80  | 60.10        | 72.20        | 99.00     | 44.80  | 61.70        |
|          | Deco        | 66.30        | 61.20     | 89.20  | 72.60        | 64.30        | 59.50     | 89.20  | 71.40        | 79.20        | 74.30     | 89.20  | 81.10        |
|          | SAVER(Ours) | 68.10        | 63.00     | 87.30  | <b>73.20</b> | <b>65.70</b> | 60.90     | 87.30  | <b>71.80</b> | <b>83.20</b> | 80.60     | 87.30  | <b>83.80</b> |
| Painting | Dola        | <b>71.40</b> | 90.70     | 47.70  | 62.50        | <b>71.90</b> | 92.70     | 47.70  | 62.90        | 73.40        | 98.40     | 47.70  | 64.20        |
|          | Deco        | 68.30        | 63.20     | 87.90  | <b>73.50</b> | 65.20        | 60.50     | 87.90  | <b>71.60</b> | 82.60        | 79.50     | 87.90  | 83.50        |
|          | SAVER(Ours) | 68.20        | 63.80     | 83.80  | 72.50        | 66.70        | 62.40     | 83.80  | 71.50        | <b>84.30</b> | 84.60     | 83.80  | <b>84.20</b> |
| Sketch   | Dola        | 69.60        | 91.90     | 42.90  | 58.50        | 70.00        | 93.70     | 42.90  | 58.80        | 71.20        | 98.70     | 42.90  | 59.80        |
|          | Deco        | 69.90        | 65.10     | 86.00  | <b>74.10</b> | 68.10        | 63.30     | 86.00  | 72.90        | 83.20        | 81.50     | 86.00  | 83.70        |
|          | SAVER(Ours) | <b>70.80</b> | 67.10     | 81.40  | 73.60        | <b>70.30</b> | 66.60     | 81.40  | <b>73.30</b> | <b>85.30</b> | 88.20     | 81.40  | <b>84.70</b> |
| Original | Dola        | <b>75.20</b> | 90.40     | 56.30  | 69.40        | 75.70        | 91.80     | 56.30  | 69.80        | 77.90        | 99.20     | 56.30  | 71.90        |
|          | Deco        | 72.60        | 68.00     | 85.60  | <b>75.80</b> | 72.10        | 67.40     | 85.60  | 75.40        | 86.30        | 86.80     | 85.60  | 86.20        |
|          | SAVER(Ours) | 73.60        | 69.80     | 83.00  | <b>75.80</b> | <b>74.10</b> | 70.50     | 83.00  | <b>76.20</b> | <b>86.90</b> | 90.10     | 83.00  | <b>86.40</b> |
| Average  | Dola        | <b>71.60</b> | 90.30     | 48.45  | 62.93        | 72.00        | 91.72     | 48.45  | 63.25        | 73.87        | 98.57     | 48.45  | 64.85        |
|          | Deco        | 68.57        | 63.62     | 87.50  | <b>73.63</b> | 66.20        | 61.53     | 87.50  | 72.17        | 81.62        | 78.62     | 87.50  | 82.72        |
|          | SAVER(Ours) | 69.45        | 64.98     | 84.82  | 73.53        | <b>68.00</b> | 63.73     | 84.82  | <b>72.67</b> | <b>84.12</b> | 83.90     | 84.82  | <b>84.25</b> |

Table 13: Style-POPE benchmark results on LLaVA-1.5.

| Style    | Method      | Adversarial  |           |        |              | Popular      |           |        |              | Random       |           |        |              |
|----------|-------------|--------------|-----------|--------|--------------|--------------|-----------|--------|--------------|--------------|-----------|--------|--------------|
|          |             | ACC          | Precision | Recall | F1           | ACC          | Precision | Recall | F1           | ACC          | Precision | Recall | F1           |
| Cartoon  | Dola        | 67.60        | 67.30     | 68.30  | 67.80        | 67.60        | 67.30     | 68.30  | 67.80        | 67.90        | 67.80     | 68.30  | 68.10        |
|          | Deco        | 64.70        | 59.40     | 93.20  | 72.50        | 66.30        | 60.60     | 93.20  | 73.40        | 73.90        | 67.20     | 93.20  | 78.10        |
|          | SAVER(Ours) | <b>70.10</b> | 64.80     | 88.10  | <b>74.70</b> | <b>73.10</b> | 67.70     | 88.10  | <b>76.60</b> | <b>81.70</b> | 78.10     | 88.10  | <b>82.80</b> |
| Game     | Dola        | 66.80        | 66.80     | 66.90  | 66.90        | 68.20        | 68.60     | 66.90  | 67.80        | 66.30        | 66.10     | 66.90  | 66.50        |
|          | Deco        | 65.70        | 60.10     | 93.20  | 73.10        | 67.20        | 61.30     | 93.20  | 74.00        | 76.60        | 70.00     | 93.20  | 79.90        |
|          | SAVER(Ours) | <b>70.20</b> | 65.00     | 87.70  | <b>74.60</b> | <b>74.20</b> | 69.00     | 87.70  | <b>77.20</b> | <b>82.90</b> | 80.10     | 87.70  | <b>83.70</b> |
| Graffiti | Dola        | 63.90        | 64.10     | 63.10  | 63.60        | 64.30        | 64.60     | 63.10  | 63.90        | 62.20        | 61.90     | 63.10  | 62.50        |
|          | Deco        | 63.30        | 58.20     | 94.10  | 71.90        | 65.80        | 60.10     | 94.10  | 73.30        | 73.30        | 66.40     | 94.10  | 77.90        |
|          | SAVER(Ours) | <b>69.30</b> | 64.20     | 87.40  | <b>74.00</b> | <b>72.50</b> | 67.30     | 87.40  | <b>76.10</b> | <b>81.80</b> | 78.60     | 87.40  | <b>82.80</b> |
| Painting | Dola        | 66.40        | 66.00     | 67.80  | 66.90        | 67.60        | 67.50     | 67.80  | 67.60        | 67.10        | 66.90     | 67.80  | 67.30        |
|          | Deco        | 66.30        | 60.70     | 92.20  | 73.20        | 68.80        | 62.80     | 92.20  | 74.70        | 78.20        | 72.00     | 92.20  | 80.90        |
|          | SAVER(Ours) | <b>70.80</b> | 66.00     | 85.60  | <b>74.50</b> | <b>74.80</b> | 70.40     | 85.60  | <b>77.20</b> | <b>83.30</b> | 81.90     | 85.60  | <b>83.70</b> |
| Sketch   | Dola        | 65.10        | 61.90     | 63.50  | 47.50        | 65.10        | 61.90     | 63.50  | 47.50        | 63.70        | 61.90     | 62.80  | 48.60        |
|          | Deco        | 66.40        | 60.70     | 93.40  | 73.60        | 70.10        | 63.70     | 93.40  | 75.80        | 78.70        | 72.20     | 93.40  | 81.50        |
|          | SAVER(Ours) | <b>72.10</b> | 66.80     | 87.70  | <b>75.80</b> | <b>75.80</b> | 70.90     | 87.70  | <b>78.40</b> | <b>84.20</b> | 81.90     | 87.70  | <b>84.70</b> |
| Original | Dola        | 69.30        | 67.80     | 73.60  | 70.60        | 70.20        | 68.90     | 73.60  | 71.10        | 71.50        | 70.70     | 73.60  | 72.10        |
|          | Deco        | 68.40        | 61.70     | 97.00  | 75.50        | 70.30        | 63.20     | 97.00  | 76.50        | 82.80        | 75.60     | 97.00  | 85.00        |
|          | SAVER(Ours) | <b>73.90</b> | 67.30     | 92.80  | <b>78.00</b> | <b>77.10</b> | 70.60     | 92.80  | <b>80.20</b> | <b>88.20</b> | 85.00     | 92.80  | <b>88.70</b> |
| Average  | Dola        | 66.52        | 65.65     | 67.20  | 63.88        | 67.17        | 66.47     | 67.20  | 64.28        | 66.45        | 65.88     | 67.08  | 64.18        |
|          | Deco        | 65.80        | 60.13     | 93.85  | 73.30        | 68.08        | 61.95     | 93.85  | 74.62        | 77.25        | 70.57     | 93.85  | 80.55        |
|          | SAVER(Ours) | <b>71.07</b> | 65.68     | 88.22  | <b>75.27</b> | <b>74.58</b> | 69.32     | 88.22  | <b>77.62</b> | <b>83.68</b> | 80.93     | 88.22  | <b>84.40</b> |

### Hallucination Evaluation Results on MME dataset

MME is a more challenging dataset for LVLM hallucination evaluation, which comprises 14 fine-grained Visual Question Answering (VQA) tasks grouped into two distinct tracks: (i) ten perception-oriented tasks evaluating fundamental visual understanding abilities such as object existence, counting, and color identification; and (ii) four recognition-oriented tasks requiring advanced reasoning abilities, including commonsense inference, numerical calculations, text translation, and code understanding. As shown in the Tabs. 4 and 14, SAVER consistently achieves the highest scores across both perception and recognition tracks, regardless of the evaluated backbone architectures. These results indicate that our method not only effectively mitigates hallucinations but also enhances general visual comprehension. This improvement can be attributed to our method leveraging more visual information aligned with the text cues.

Table 14: Results on MME perception-related tasks. The best performance of each setting is bolded.

| Model        | Method      | Existence    | Count        | Position     | Color        | Posters      | Celebrity    | Scene        | Landmark     | Artwork      | OCR          | Total Score   |
|--------------|-------------|--------------|--------------|--------------|--------------|--------------|--------------|--------------|--------------|--------------|--------------|---------------|
| LLaVA-1.5    | Dola        | 170.0        | 55.0         | <b>126.7</b> | 108.3        | 79.3         | 69.1         | 117.8        | 114.0        | <b>76.0</b>  | 25.0         | 941.1         |
|              | Deco        | 165.0        | 93.3         | 91.7         | 95.0         | 138.8        | 103.5        | 151.5        | 112.0        | 58.3         | 85.0         | 1094.1        |
|              | SAVER(Ours) | <b>185.0</b> | <b>113.3</b> | 106.7        | <b>125.0</b> | <b>144.9</b> | <b>117.4</b> | <b>155.3</b> | <b>134.8</b> | 66.0         | <b>117.5</b> | <b>1265.8</b> |
| InstructBLIP | Dola        | 165.0        | 68.3         | 50.0         | <b>148.3</b> | 60.2         | 60.2         | 110.0        | 50.0         | 87.8         | 87.5         | 876.8         |
|              | Deco        | <b>190.0</b> | 60.0         | 58.3         | 115.0        | 138.8        | 128.2        | 151.5        | <b>107.8</b> | 113.8        | <b>125.0</b> | 1188.3        |
|              | SAVER(Ours) | <b>190.0</b> | <b>85.0</b>  | <b>66.7</b>  | 100.0        | <b>142.5</b> | <b>147.6</b> | <b>158.0</b> | 96.5         | <b>132.5</b> | 95.0         | <b>1213.8</b> |

### Real-World Cases

**Benchmark Details.** To evaluate SAVER in more practical cases, we first collect a cross-modal dataset from three public datasets:

- **Depth-RGB (100 pairs).** Indoor scenes from NYU-Depth (Silberman et al. 2012); each dense depth map ( $640 \times 480$ ) is aligned with a RGB photograph captured from the same viewpoint.
- **Thermal-RGB (100 pairs).** Thermal and RGB frames from the KAIST Multispectral Pedestrian Benchmark (Hwang et al. 2015); each long-wave infrared image ( $640 \times 512$ ) has a pixel-wise registered RGB counterpart.
- **Medical (50 images).** Single-channel X-rays from BenchLLM (Cai et al. 2024).

Following POPE, we formulate hallucination detection as a binary VQA task. For each image, we pose a concise, domain-specific “Yes/No” query that targets an object:

Table 15: Results on Depth, Thermal, and Medical images.

| Style       | Method | LLaVA-1.5   |             | MiniGPT-4   |             | InstructBLIP |             |
|-------------|--------|-------------|-------------|-------------|-------------|--------------|-------------|
|             |        | ACC         | F1          | ACC         | F1          | ACC          | F1          |
| Depth       | Dola   | 51.0        | 47.3        | 54.0        | 23.3        | 50.0         | 0.0         |
|             | Deco   | 57.0        | 67.2        | 49.0        | 65.3        | 49.0         | 55.7        |
|             | Ours   | 61.0        | 66.7        | 48.0        | 63.4        | 50.0         | 41.9        |
| Depth-RGB   | Dola   | 64.0        | 70.0        | 54.0        | 45.2        | 65.0         | 47.8        |
|             | Deco   | 57.0        | 69.9        | 52.0        | 67.6        | 70.0         | 72.7        |
|             | Ours   | 63.0        | 72.6        | 51.0        | 66.2        | 82.0         | 82.4        |
| Thermal     | Dola   | 64.0        | 69.5        | 56.0        | 52.2        | 79.0         | 77.9        |
|             | Deco   | 65.0        | 73.7        | 50.0        | 66.7        | 59.0         | 70.5        |
|             | Ours   | 71.0        | 76.4        | 50.0        | 66.7        | 64.0         | 73.1        |
| Thermal-RGB | Dola   | 76.0        | 80.0        | 63.0        | 65.4        | 85.0         | 86.0        |
|             | Deco   | 58.0        | 69.6        | 50.0        | 66.7        | 60.0         | 71.4        |
|             | Ours   | 71.0        | 76.4        | 60.0        | 70.6        | 65.0         | 73.7        |
| Medical     | Dola   | 56.0        | 45.0        | 50.0        | 0.0         | 50.0         | 7.4         |
|             | Deco   | 50.0        | 66.7        | 50.0        | 65.8        | 62.0         | 70.8        |
|             | Ours   | 54.0        | 66.7        | 48.0        | 64.9        | 64.0         | 71.9        |
| Average     | Dola   | 62.2        | 62.4        | <b>55.4</b> | 37.2        | <b>65.8</b>  | 43.8        |
|             | Deco   | 57.4        | 69.4        | 50.2        | <b>66.4</b> | 60.0         | 68.2        |
|             | Ours   | <b>64.0</b> | <b>71.8</b> | 51.4        | <b>66.4</b> | 65.0         | <b>68.6</b> |

| Modality | Prompt (example)                         |
|----------|--|
| Thermal  | <i>“Is there a person in the image?”</i> |
| Depth    | <i>“Is there a laptop on the desk?”</i>  |
| Medical  | <i>“Does the picture contain lungs?”</i> |

Objects are selected to (i) exhibit clear visual signatures when present, (ii) occur frequently in text-only corpora to align with real-world scenarios, and (iii) target the specific practical usage. This benchmark comprises 450 images paired with corresponding “Yes/No” queries, providing a rigorous test of LVLM robustness against hallucination. Some example images are shown in Fig. 7.

**Experiments on Real-World Benchmark.** Tab. 15 reports results on five real-world modalities—*Depth*, *Depth-RGB*, *Thermal*, *Thermal-RGB*, and *Medical*—evaluated with three LVLMs: LLaVA-1.5 (Liu et al. 2024b), MiniGPT-4 (Zhu et al. 2023), and InstructBLIP (Dai et al. 2023). We compare our **SAVER** with two baseline hallucination mitigation approaches, Dola (Chuang et al. 2023) and Deco (Wang et al. 2024a). SAVER exhibits the highest F1 scores under various experimental settings. These findings further demonstrate that our method can be effectively extended to challenging real-world data for hallucination mitigation.

## Ablation Study on Hyperparameters

Here, we present the detailed ablation studies on five key hyperparameters. The average results are illustrated in Fig. 6, and The detailed results can be found in Tabs. 16, 17, and 18.

**Effect of the Scale Factor  $\alpha$ .** Tuning the scale factor  $\alpha \in \{0.4, 0.6, 0.8, 1.0\}$  modulates the contribution of visual evidence in the fused representation. Higher values of  $\alpha$  enhance visual guidance and generally reduce hallucinations; however, large values occasionally result in overly constrained generation.

**Effect of the Confidence Threshold  $p$ .** The confidence threshold  $p \in \{0.6, 0.7, 0.8, 0.9\}$  controls token selection by filtering candidate tokens based on confidence. Higher thresholds more aggressively suppress hallucinations but may remove relevant content, adversely affecting fluency. Tab. 17 demonstrates this trade-off, where lower thresholds ( $p = 0.6$ ) yield fewer hallucinations on stylized inputs, whereas intermediate to high thresholds ( $p = 0.8\text{--}0.9$ ) perform optimally on Original images. This pattern is most evident with MiniGPT-4 and InstructBLIP, suggesting mid-range  $p$  provides an optimal balance between robustness and fluency.

**Effect of the Candidate Set Size  $k$ .** We also examine the effect of the number of candidate tokens  $k \in \{10, 15, 20, 25\}$ . Low  $k$  value excludes potentially informative tokens, hindering performance on rare styles, while excessively high  $k$  introduces noisy tokens. From Tabs. 16, 17, and 18, we consistently observe optimal performance at  $k = 20$ , achieving the lowest average hallucination counts (e.g., LLaVA-1.5 in Tab. 18).

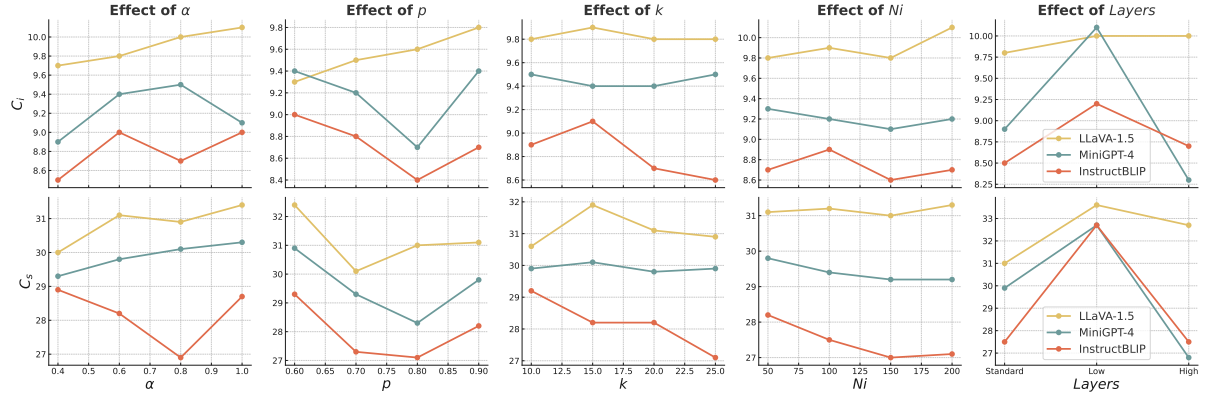


Figure 6: Ablation studies on hyperparameters.



Figure 7: Example images of Real-World Cases. Left: Thermal-RGB images, middle: Depth-RGB images, and Right: Medical images.

**Effect of Candidate Image Representative Tokens  $N_i$ .** We adjust the number of candidate image representations  $N_i \in \{50, 100, 150, 200\}$  to assess its influence. Moderate values ( $N_i = 50$  or  $100$ ) consistently provide the best trade-off by ensuring sufficient diversity to mitigate hallucinations during the decoding process (Tab. 17, LLaVA-1.5). Higher values ( $N_i \geq 150$ ) rarely yield further improvements.

**Interaction with Early-Exit Depth.** Following (Wang et al. 2024a), we adopt the same layer configuration (20-29 layers) as the “Standard” and investigate two alternative exit strategies: Extract 10 layers at equal intervals with in the early 20 layers (*low*) and final 20 layers (*high*), to evaluate the impact of depth. The “Standard” policy consistently achieves the best overall hallucination mitigation results on stylized inputs. Notably, the higher layer exhibits better hallucination suppression.

## Qualitative Results

To qualitatively assess the responses produced by different models and decoding strategies, we present qualitative examples in Figs. 8, 9, and 10. Compared to SOTA methods, **SAVER** generates captions that maintain more descriptive detail and length while remarkably reducing object hallucinations.

## Hardware Setup

We run our benchmark and decoding method comparison experiments using one NVIDIA A40 GPU with 48 GB memory.

Table 16: Ablation studies on the hyper-parameters of SAVER with “*Standard*” early exit layers, including the number of candidate tokens  $k$ , the scale factor  $\alpha$ , the number of candidate image representations  $N_i$ , and the threshold  $p$ . CHAIRs and CHAIRi are denoted as Cs and Ci. Lower Cs and Ci indicate fewer hallucinations.

| Model        | $\alpha$ | $N_i$ | $k$ | $p$ | Cartoon     |             | Game       |             | Graffiti    |             | Painting   |             | Sketch      |             | Original   |             | Average    |             |
|--------------|----------|-------|-----|-----|-------------|-------------|------------|-------------|-------------|-------------|------------|-------------|-------------|-------------|------------|-------------|------------|-------------|
|              |          |       |     |     | Ci          | Cs          | Ci         | Cs          | Ci          | Cs          | Ci         | Cs          | Ci          | Cs          | Ci         | Cs          | Ci         | Cs          |
| LLaVA-1.5    | 0.4      | 50    | 20  | 0.9 | 11.2        | 32.7        | <b>8.8</b> | 29.7        | 11.4        | <b>30.3</b> | 9.3        | <b>29.0</b> | <b>10.6</b> | <b>32.0</b> | <b>6.6</b> | 26.0        | <b>9.7</b> | <b>30.0</b> |
|              | 0.6      | 50    | 20  | 0.9 | <b>10.3</b> | <b>32.0</b> | 9.2        | 30.7        | <b>11.3</b> | 30.7        | <b>9.1</b> | 30.7        | 11.7        | 35.0        | 7.2        | 27.7        | 9.8        | 31.1        |
|              | 0.8      | 50    | 20  | 0.9 | 10.9        | 33.3        | 9.2        | 29.7        | 11.6        | 32.3        | 10.0       | 30.7        | 11.1        | 34.3        | 6.9        | <b>25.3</b> | 10.0       | 30.9        |
|              | 1.0      | 50    | 20  | 0.9 | 10.5        | 33.7        | 9.0        | <b>29.0</b> | 12.5        | 34.7        | 10.3       | 32.0        | 10.8        | 33.7        | 7.2        | <b>25.3</b> | 10.1       | 31.4        |
|              | 0.6      | 50    | 20  | 0.6 | 10.5        | 38.0        | 8.7        | 30.7        | 11.3        | 35.0        | <b>8.7</b> | 30.7        | <b>9.7</b>  | 32.0        | 6.8        | 27.7        | <b>9.3</b> | 32.4        |
|              | 0.6      | 50    | 20  | 0.7 | 11.9        | 35.3        | 8.8        | <b>29.3</b> | <b>10.6</b> | 31.0        | 8.8        | <b>27.3</b> | 10.1        | <b>31.7</b> | <b>6.7</b> | <b>26.0</b> | 9.5        | <b>30.1</b> |
|              | 0.6      | 50    | 20  | 0.8 | 11.3        | 36.0        | <b>8.3</b> | <b>29.3</b> | 11.4        | 32.0        | 9.5        | 29.3        | 10.2        | 32.3        | 6.8        | 27.3        | 9.6        | 31.0        |
|              | 0.6      | 50    | 20  | 0.9 | <b>10.3</b> | <b>32.0</b> | 9.2        | 30.7        | 11.3        | <b>30.7</b> | 9.1        | 30.7        | 11.7        | 35.0        | 7.2        | 27.7        | 9.8        | 31.1        |
|              | 0.6      | 50    | 10  | 0.9 | 11.1        | 33.0        | 9.2        | 31.7        | <b>10.6</b> | 31.0        | 10.4       | 31.3        | <b>10.6</b> | <b>31.3</b> | <b>6.9</b> | <b>25.3</b> | <b>9.8</b> | 30.6        |
|              | 0.6      | 50    | 15  | 0.9 | 11.2        | 34.0        | 8.9        | 30.0        | 10.8        | <b>30.7</b> | 9.5        | 31.0        | 11.5        | 38.3        | 7.5        | 27.3        | 9.9        | 31.9        |
|              | 0.6      | 50    | 20  | 0.9 | <b>10.3</b> | <b>32.0</b> | 9.2        | 30.7        | 11.3        | <b>30.7</b> | 9.1        | 30.7        | 11.7        | 35.0        | 7.2        | 27.7        | <b>9.8</b> | 31.1        |
|              | 0.6      | 50    | 25  | 0.9 | 10.9        | 33.3        | <b>8.8</b> | <b>28.7</b> | 11.6        | 31.7        | <b>8.7</b> | <b>28.7</b> | 11.7        | 35.7        | 7.3        | 27.3        | <b>9.8</b> | 30.9        |
|              | 0.6      | 50    | 20  | 0.9 | <b>10.3</b> | <b>32.0</b> | 9.2        | 30.7        | <b>11.3</b> | <b>30.7</b> | <b>9.1</b> | 30.7        | 11.7        | 35.0        | 7.2        | 27.7        | <b>9.8</b> | 31.1        |
|              | 0.6      | 100   | 20  | 0.9 | 10.8        | 33.3        | <b>8.9</b> | <b>28.7</b> | 12.0        | 33.3        | 9.2        | <b>28.7</b> | 11.7        | 36.3        | <b>6.8</b> | 27.0        | 9.9        | 31.2        |
|              | 0.6      | 150   | 20  | 0.9 | 10.8        | 33.3        | 9.3        | 29.7        | 11.7        | 33.3        | <b>9.1</b> | 30.3        | <b>11.3</b> | <b>34.3</b> | <b>6.8</b> | <b>25.3</b> | <b>9.8</b> | <b>31.0</b> |
|              | 0.6      | 200   | 20  | 0.9 | 10.8        | 33.3        | 9.4        | 30.0        | 11.9        | 33.3        | 9.4        | 29.3        | 11.7        | 35.7        | 7.2        | 26.3        | 10.1       | 31.3        |
| MiniGPT-4    | 0.4      | 50    | 20  | 0.9 | <b>10.3</b> | <b>32.7</b> | <b>8.3</b> | <b>28.7</b> | <b>10.4</b> | 29.3        | 8.6        | 30.0        | <b>8.7</b>  | 29.0        | 7.2        | 26.0        | <b>8.9</b> | <b>29.3</b> |
|              | 0.6      | 50    | 20  | 0.9 | 12.5        | 34.3        | 8.8        | 31.3        | <b>10.4</b> | 29.0        | 9.2        | 30.0        | <b>8.7</b>  | 27.7        | 6.8        | 26.3        | 9.4        | 29.8        |
|              | 0.8      | 50    | 20  | 0.9 | 11.9        | 36.7        | 9.6        | 33.7        | 11.0        | <b>28.3</b> | 8.7        | 29.0        | 9.0         | <b>27.0</b> | 6.8        | 25.7        | 9.5        | 30.1        |
|              | 1.0      | 50    | 20  | 0.9 | 11.1        | 37.0        | 9.5        | 33.3        | 10.5        | 29.7        | <b>8.3</b> | <b>28.7</b> | 8.9         | 28.0        | <b>6.5</b> | <b>25.0</b> | 9.1        | 30.3        |
|              | 0.6      | 50    | 20  | 0.6 | 10.5        | 34.0        | 9.3        | <b>30.0</b> | <b>10.2</b> | 30.7        | 8.9        | 27.7        | 10.0        | 35.3        | 7.4        | 27.7        | 9.4        | 30.9        |
|              | 0.6      | 50    | 20  | 0.7 | 10.2        | 32.7        | 8.9        | 30.7        | 11.0        | 29.3        | 8.7        | 27.3        | 10.1        | 31.7        | <b>6.3</b> | <b>24.3</b> | 9.2        | 29.3        |
|              | 0.6      | 50    | 20  | 0.8 | <b>9.9</b>  | <b>32.0</b> | <b>8.5</b> | 30.3        | 10.8        | <b>28.3</b> | <b>7.7</b> | <b>26.3</b> | <b>8.6</b>  | 28.0        | 6.5        | 25.0        | <b>8.7</b> | <b>28.3</b> |
|              | 0.6      | 50    | 20  | 0.9 | 12.5        | 34.3        | 8.8        | 31.3        | 10.4        | 29.0        | 9.2        | 30.0        | 8.7         | <b>27.7</b> | 6.8        | 26.3        | 9.4        | 29.8        |
|              | 0.6      | 50    | 10  | 0.9 | <b>11.4</b> | <b>34.0</b> | 9.0        | 32.0        | 11.1        | <b>28.7</b> | 9.7        | 30.7        | 8.6         | 27.7        | 6.9        | 26.3        | 9.5        | 29.9        |
|              | 0.6      | 50    | 15  | 0.9 | 11.5        | 34.3        | <b>8.8</b> | 31.7        | 10.9        | 29.3        | 9.3        | 31.0        | 8.8         | 28.7        | 6.9        | <b>25.3</b> | <b>9.4</b> | 30.1        |
|              | 0.6      | 50    | 20  | 0.9 | 12.5        | 34.3        | <b>8.8</b> | <b>31.3</b> | <b>10.4</b> | 29.0        | 9.2        | <b>30.0</b> | 8.7         | 27.7        | <b>6.8</b> | 26.3        | <b>9.4</b> | <b>29.8</b> |
|              | 0.6      | 50    | 25  | 0.9 | 12.9        | 35.0        | <b>8.8</b> | 32.0        | 10.9        | 30.3        | <b>9.1</b> | <b>30.0</b> | <b>8.4</b>  | <b>27.0</b> | 6.9        | <b>25.3</b> | 9.5        | 29.9        |
|              | 0.6      | 50    | 20  | 0.9 | 12.5        | 34.3        | 8.8        | 31.3        | 10.4        | 29.0        | 9.2        | 30.0        | <b>8.7</b>  | 27.7        | 6.8        | 26.3        | 9.4        | 29.8        |
|              | 0.6      | 100   | 20  | 0.9 | 12.2        | 33.3        | 8.4        | 30.3        | 10.4        | <b>28.7</b> | 8.7        | 29.7        | 8.9         | 28.3        | 6.7        | 26.0        | 9.2        | 29.4        |
|              | 0.6      | 150   | 20  | 0.9 | 12.1        | 33.3        | <b>8.3</b> | <b>30.0</b> | <b>10.3</b> | <b>28.7</b> | <b>8.4</b> | <b>29.0</b> | 8.9         | 28.7        | <b>6.6</b> | <b>25.7</b> | <b>9.1</b> | <b>29.2</b> |
|              | 0.6      | 200   | 20  | 0.9 | <b>12.0</b> | <b>33.0</b> | 8.5        | 30.7        | <b>10.3</b> | <b>28.7</b> | 8.6        | 29.7        | 8.9         | <b>27.3</b> | 6.7        | 26.0        | 9.2        | <b>29.2</b> |
| InstructBLIP | 0.4      | 50    | 20  | 0.9 | 10.2        | 33.7        | <b>7.8</b> | 29.0        | 9.9         | 30.0        | 8.6        | 27.7        | <b>8.5</b>  | <b>28.7</b> | <b>6.1</b> | 24.0        | <b>8.5</b> | 28.9        |
|              | 0.6      | 50    | 20  | 0.9 | <b>10.0</b> | <b>32.7</b> | 8.1        | 28.0        | 9.6         | 28.3        | 8.4        | 26.0        | 8.8         | 29.0        | <b>6.1</b> | 25.3        | <b>8.5</b> | 28.2        |
|              | 0.8      | 50    | 20  | 0.9 | 10.6        | <b>32.7</b> | <b>7.8</b> | <b>27.0</b> | <b>9.3</b>  | <b>26.3</b> | <b>8.2</b> | <b>24.3</b> | 9.6         | 29.0        | <b>6.1</b> | <b>22.3</b> | 8.6        | <b>26.9</b> |
|              | 1.0      | 50    | 20  | 0.9 | 10.7        | 33.7        | 8.2        | 28.7        | 10.6        | 29.3        | 9.0        | 27.3        | 9.0         | 29.3        | 6.3        | 23.7        | 9.0        | 28.7        |
|              | 0.6      | 50    | 20  | 0.6 | 10.3        | 36.3        | 8.2        | 29.3        | <b>8.8</b>  | 29.3        | 8.4        | 28.3        | 7.6         | 30.3        | 5.5        | 22.0        | 8.1        | 29.3        |
|              | 0.6      | 50    | 20  | 0.7 | 9.9         | <b>32.0</b> | 8.0        | 30.0        | 9.9         | <b>28.0</b> | <b>7.4</b> | <b>25.3</b> | 7.8         | <b>27.0</b> | <b>5.3</b> | 21.3        | 8.1        | 27.3        |
|              | 0.6      | 50    | 20  | 0.8 | <b>9.2</b>  | 32.7        | <b>7.7</b> | <b>26.3</b> | 9.4         | <b>28.0</b> | 8.5        | 25.7        | <b>7.3</b>  | 28.7        | 5.8        | <b>21.0</b> | <b>8.0</b> | <b>27.1</b> |
|              | 0.6      | 50    | 20  | 0.9 | 10.0        | 32.7        | 8.1        | 28.0        | 9.6         | 28.3        | 8.4        | 26.0        | 8.8         | 29.0        | 6.1        | 25.3        | 8.5        | 28.2        |
|              | 0.6      | 50    | 10  | 0.9 | 10.9        | 34.3        | 8.4        | 27.3        | 10.6        | 31.7        | 8.5        | 27.0        | 8.3         | 30.0        | 6.5        | 25.0        | 8.9        | 29.2        |
|              | 0.6      | 50    | 15  | 0.9 | 10.6        | 33.3        | 8.0        | 29.7        | 10.2        | 30.3        | 8.7        | 27.3        | 8.1         | <b>25.3</b> | <b>5.9</b> | <b>23.0</b> | 8.6        | 28.2        |
|              | 0.6      | 50    | 20  | 0.9 | 10.0        | 32.7        | 8.1        | 28.0        | 9.6         | 28.3        | 8.4        | 26.0        | 8.8         | 29.0        | 6.1        | 25.3        | 8.5        | 28.2        |
|              | 0.6      | 50    | 25  | 0.9 | <b>9.7</b>  | <b>32.3</b> | <b>7.3</b> | <b>26.7</b> | <b>9.2</b>  | <b>26.3</b> | <b>8.0</b> | <b>24.0</b> | <b>7.7</b>  | 27.0        | 6.4        | 26.3        | <b>8.1</b> | <b>27.1</b> |
|              | 0.6      | 50    | 20  | 0.9 | 10.0        | 32.7        | 8.1        | 28.0        | 9.6         | 28.3        | 8.4        | 26.0        | 8.8         | 29.0        | <b>6.1</b> | 25.3        | 8.5        | 28.2        |
|              | 0.6      | 100   | 20  | 0.9 | <b>9.6</b>  | 31.7        | 9.5        | 27.0        | <b>9.5</b>  | <b>27.0</b> | 8.9        | 27.0        | <b>7.1</b>  | <b>26.7</b> | 6.2        | 25.3        | 8.5        | 27.5        |
|              | 0.6      | 150   | 20  | 0.9 | 9.9         | 31.0        | 7.4        | 25.7        | 10.2        | 27.7        | 8.4        | 26.7        | 8.2         | <b>26.7</b> | 6.3        | 24.3        | 8.4        | <b>27.0</b> |
|              | 0.6      | 200   | 20  | 0.9 | 9.7         | <b>30.7</b> | <b>7.2</b> | <b>25.3</b> | 9.8         | 28.7        | <b>8.3</b> | 26.3        | 8.4         | 27.3        | 6.2        | <b>24.0</b> | <b>8.3</b> | 27.1        |

Table 17: Ablation studies on the hyper-parameters of SAVER with “*Low*” early exit layers, including the number of candidate tokens  $k$ , the scale factor  $\alpha$ , the number of candidate image representations  $N_i$ , and the threshold  $p$ . CHAIRs and CHAIRi are denoted as Cs and Ci. Lower Cs and Ci indicate fewer hallucinations.

| Model        | $\alpha$ | $N_i$ | $k$ | $p$ | Cartoon     |             | Game        |             | Graffiti    |             | Painting    |             | Sketch      |             | Original   |             | Average     |             |
|--------------|----------|-------|-----|-----|-------------|-------------|-------------|-------------|-------------|-------------|-------------|-------------|-------------|-------------|------------|-------------|-------------|-------------|
|              |          |       |     |     | Ci          | Cs          | Ci         | Cs          | Ci          | Cs          |
| LLaVA-1.5    | 0.4      | 50    | 20  | 0.9 | 10.8        | 36.3        | 9.6         | 33.7        | <b>10.5</b> | 35.0        | 10.5        | 34.3        | <b>9.4</b>  | <b>32.0</b> | 7.5        | 29.3        | 9.7         | 33.4        |
|              | 0.6      | 50    | 20  | 0.9 | 11.5        | 39.3        | 9.4         | 34.3        | 11.3        | 35.0        | 10.5        | 34.7        | 9.9         | <b>32.0</b> | <b>7.1</b> | <b>28.3</b> | 10.0        | 33.9        |
|              | 0.8      | 50    | 20  | 0.9 | 11.2        | 39.3        | <b>8.9</b>  | 31.7        | 12.2        | 37.0        | 10.7        | 34.7        | 10.1        | 32.3        | 7.8        | 30.0        | 10.2        | 34.2        |
|              | 1.0      | 50    | 20  | 0.9 | <b>10.2</b> | <b>35.7</b> | <b>8.9</b>  | <b>31.3</b> | 11.1        | <b>33.3</b> | <b>10.4</b> | <b>32.0</b> | 10.1        | 33.3        | <b>7.1</b> | 28.7        | <b>9.6</b>  | <b>32.4</b> |
|              | 0.6      | 50    | 20  | 0.6 | <b>10.5</b> | <b>35.7</b> | <b>8.7</b>  | <b>30.3</b> | <b>10.6</b> | 34.0        | 10.7        | 34.3        | 10.9        | 35.3        | 7.0        | 30.0        | <b>9.7</b>  | 33.3        |
|              | 0.6      | 50    | 20  | 0.7 | 11.5        | 37.0        | 8.9         | 34.0        | 10.7        | 33.3        | 11.0        | <b>33.3</b> | 10.1        | 34.0        | <b>6.7</b> | 28.7        | 9.8         | 33.4        |
|              | 0.6      | 50    | 20  | 0.8 | 12.4        | 37.7        | 9.3         | 32.7        | 10.7        | <b>33.0</b> | 11.2        | 35.3        | <b>9.7</b>  | <b>31.7</b> | 7.3        | 28.7        | 10.1        | <b>33.2</b> |
|              | 0.6      | 50    | 20  | 0.9 | 11.5        | 39.3        | 9.4         | 34.3        | 11.3        | 35.0        | <b>10.5</b> | 34.7        | 9.9         | 32.0        | 7.1        | <b>28.3</b> | 10.0        | 33.9        |
|              | 0.6      | 50    | 10  | 0.9 | <b>10.6</b> | <b>36.3</b> | 9.9         | 34.3        | <b>10.2</b> | <b>33.0</b> | 11.4        | <b>33.7</b> | 10.5        | 35.3        | 7.9        | 29.7        | 10.1        | 33.7        |
|              | 0.6      | 50    | 15  | 0.9 | 11.6        | 39.7        | 9.5         | <b>33.0</b> | 10.7        | 34.3        | 11.1        | 34.7        | 10.3        | 33.0        | <b>7.0</b> | <b>27.0</b> | <b>10.0</b> | <b>33.6</b> |
|              | 0.6      | 50    | 20  | 0.9 | 11.5        | 39.3        | <b>9.4</b>  | 34.3        | 11.3        | 35.0        | <b>10.5</b> | 34.7        | 9.9         | 32.0        | 7.1        | 28.3        | <b>10.0</b> | 33.9        |
|              | 0.6      | 50    | 25  | 0.9 | 12.0        | 40.0        | <b>9.4</b>  | 33.7        | 11.8        | 36.3        | 11.1        | 36.3        | <b>9.6</b>  | <b>31.3</b> | 7.9        | 30.7        | 10.3        | 34.7        |
| MiniGPT-4    | 0.6      | 50    | 20  | 0.9 | 11.5        | 39.3        | <b>9.4</b>  | 34.3        | 11.3        | 35.0        | 10.5        | 34.7        | 9.9         | 32.0        | 7.1        | 28.3        | 10.0        | 33.9        |
|              | 0.6      | 100   | 20  | 0.9 | <b>11.2</b> | 37.7        | 10.4        | 36.6        | 11.2        | 37.7        | <b>9.8</b>  | 35.0        | 10.0        | 32.3        | 7.6        | 28.3        | 10.0        | 34.6        |
|              | 0.6      | 150   | 20  | 0.9 | 11.7        | <b>35.7</b> | 9.7         | <b>33.7</b> | <b>10.2</b> | <b>30.3</b> | 10.4        | <b>33.7</b> | 10.1        | 34.3        | <b>6.5</b> | <b>25.3</b> | <b>9.8</b>  | <b>32.2</b> |
|              | 0.6      | 200   | 20  | 0.9 | 11.6        | <b>35.7</b> | 9.9         | 34.3        | 10.8        | 33.3        | 10.9        | 38.0        | <b>9.1</b>  | <b>30.0</b> | 7.1        | 28.3        | 9.9         | 33.3        |
|              | 0.4      | 50    | 20  | 0.9 | 11.6        | 34.7        | 10.0        | <b>31.3</b> | <b>9.7</b>  | 31.0        | 9.8         | 32.3        | <b>10.8</b> | <b>35.0</b> | <b>7.4</b> | <b>29.0</b> | <b>9.9</b>  | <b>32.2</b> |
|              | 0.6      | 50    | 20  | 0.9 | <b>11.2</b> | <b>34.0</b> | 10.2        | 32.7        | 10.3        | <b>30.7</b> | 10.2        | 32.3        | 11.2        | 36.3        | 7.6        | 29.3        | 10.1        | 32.6        |
|              | 0.8      | 50    | 20  | 0.9 | 11.8        | 34.7        | <b>9.9</b>  | 33.0        | 10.8        | 31.7        | 10.1        | 31.7        | 11.3        | 36.7        | 7.8        | 29.3        | 10.3        | 32.9        |
|              | 1.0      | 50    | 20  | 0.9 | 12.1        | 35.7        | 10.0        | 33.0        | 10.9        | 31.7        | <b>9.6</b>  | <b>30.3</b> | 11.5        | 36.7        | 7.5        | 29.3        | 10.3        | 32.8        |
|              | 0.6      | 50    | 20  | 0.6 | 12.1        | 36.3        | <b>9.5</b>  | <b>31.3</b> | <b>10.3</b> | 31.7        | <b>9.5</b>  | <b>30.3</b> | <b>10.1</b> | <b>34.0</b> | 8.5        | 31.3        | <b>10.0</b> | <b>32.5</b> |
|              | 0.6      | 50    | 20  | 0.7 | 11.5        | 36.0        | 9.7         | 32.3        | 10.4        | <b>30.3</b> | 9.6         | 31.7        | 11.0        | 36.0        | 7.9        | 30.0        | <b>10.0</b> | 32.7        |
|              | 0.6      | 50    | 20  | 0.8 | <b>11.2</b> | 36.0        | 10.6        | 32.3        | 10.6        | 32.3        | 10.6        | 34.0        | 11.2        | 36.0        | 7.8        | <b>28.0</b> | 10.3        | 33.1        |
|              | 0.6      | 50    | 20  | 0.9 | <b>11.2</b> | <b>34.0</b> | 10.2        | 32.7        | <b>10.3</b> | 30.7        | 10.2        | 32.3        | 11.2        | 36.3        | <b>7.6</b> | 29.3        | 10.1        | 32.6        |
| InstructBLIP | 0.6      | 50    | 10  | 0.9 | <b>10.6</b> | <b>32.7</b> | 10.5        | 34.0        | <b>10.3</b> | 31.3        | 10.2        | 32.7        | 11.4        | 37.0        | 7.8        | <b>29.3</b> | <b>10.1</b> | 32.8        |
|              | 0.6      | 50    | 15  | 0.9 | 11.2        | 34.7        | 10.3        | 33.7        | 10.6        | 32.0        | <b>10.1</b> | 32.7        | 11.4        | 36.7        | <b>7.6</b> | 39.3        | 10.2        | 34.9        |
|              | 0.6      | 50    | 20  | 0.9 | 11.2        | 34.0        | <b>10.2</b> | <b>32.7</b> | <b>10.3</b> | <b>30.7</b> | 10.2        | 32.3        | <b>11.2</b> | 36.3        | <b>7.6</b> | <b>29.3</b> | <b>10.1</b> | <b>32.6</b> |
|              | 0.6      | 50    | 25  | 0.9 | 11.3        | 34.0        | <b>10.2</b> | <b>32.7</b> | 10.5        | 31.7        | <b>10.1</b> | <b>32.0</b> | <b>11.2</b> | <b>36.0</b> | 7.7        | 29.7        | 10.2        | 32.7        |
|              | 0.6      | 50    | 20  | 0.9 | <b>11.2</b> | <b>34.0</b> | 10.2        | 32.7        | 10.3        | <b>30.7</b> | 10.2        | 32.3        | <b>11.2</b> | <b>36.3</b> | 7.6        | 29.3        | 10.1        | 32.6        |
|              | 0.6      | 100   | 20  | 0.9 | 11.3        | 35.3        | 10.2        | 33.0        | 10.4        | <b>30.7</b> | 11.1        | 32.7        | <b>11.2</b> | 37.0        | 7.4        | 28.7        | 10.3        | 32.9        |
|              | 0.6      | 150   | 20  | 0.9 | 11.4        | 36.0        | 10.0        | 32.3        | <b>10.2</b> | <b>30.7</b> | <b>10.1</b> | 32.7        | <b>11.2</b> | 37.0        | 7.4        | <b>28.0</b> | 10.1        | 32.8        |
|              | 0.6      | 200   | 20  | 0.9 | 11.4        | 35.7        | <b>9.9</b>  | <b>32.0</b> | <b>10.2</b> | <b>30.7</b> | <b>10.1</b> | <b>32.0</b> | <b>11.2</b> | 36.7        | <b>7.3</b> | <b>28.0</b> | <b>10.0</b> | <b>32.5</b> |
|              | 0.4      | 50    | 20  | 0.9 | 11.1        | <b>36.3</b> | 10.0        | 35.3        | 11.6        | 35.7        | 7.7         | 29.0        | 9.2         | 33.7        | 6.8        | 28.3        | 9.4         | 33.1        |
|              | 0.6      | 50    | 20  | 0.9 | 11.2        | 37.3        | 9.3         | 35.0        | 11.3        | <b>33.7</b> | 7.7         | 29.0        | 8.7         | 33.3        | 7.0        | 28.0        | 9.2         | 32.7        |
|              | 0.8      | 50    | 20  | 0.9 | <b>11.0</b> | 37.7        | 9.0         | 34.0        | 10.8        | 34.3        | <b>6.8</b>  | <b>25.0</b> | 8.5         | <b>31.7</b> | <b>6.4</b> | <b>26.0</b> | 8.8         | 31.5        |
|              | 1.0      | 50    | 20  | 0.9 | 11.3        | 39.3        | <b>8.8</b>  | <b>31.3</b> | <b>10.6</b> | <b>33.7</b> | 7.7         | 28.3        | <b>8.2</b>  | <b>31.7</b> | 6.6        | 26.3        | 8.9         | 31.8        |
| InstructBLIP | 0.6      | 50    | 20  | 0.6 | 11.1        | 36.3        | <b>8.2</b>  | <b>30.3</b> | 10.3        | 32.7        | 7.0         | 27.0        | 9.3         | 34.0        | 6.4        | 25.3        | 8.7         | <b>30.9</b> |
|              | 0.6      | 50    | 20  | 0.7 | <b>10.3</b> | <b>36.0</b> | 9.0         | 34.7        | <b>9.6</b>  | <b>30.7</b> | <b>6.5</b>  | <b>24.3</b> | 8.8         | 34.7        | 6.2        | 25.0        | <b>8.4</b>  | <b>30.9</b> |
|              | 0.6      | 50    | 20  | 0.8 | 12.0        | 41.0        | 8.8         | 30.7        | 11.3        | 36.7        | 8.0         | 29.3        | <b>7.9</b>  | <b>32.0</b> | <b>6.1</b> | <b>24.7</b> | 9.0         | 32.4        |
|              | 0.6      | 50    | 20  | 0.9 | 11.2        | 37.3        | 9.3         | 35.0        | 11.3        | 33.7        | 7.7         | 29.0        | 8.7         | 33.3        | 7.0        | 28.0        | 9.2         | 32.7        |
|              | 0.6      | 50    | 10  | 0.9 | 11.8        | 37.7        | 9.4         | <b>34.3</b> | 11.6        | 35.0        | <b>7.2</b>  | <b>25.3</b> | 9.5         | 33.3        | 7.3        | 29.0        | 9.5         | <b>32.4</b> |
|              | 0.6      | 50    | 15  | 0.9 | 12.1        | 40.0        | 9.4         | 35.7        | 11.5        | 34.3        | 7.7         | 28.7        | 8.7         | 31.7        | 6.7        | <b>25.7</b> | 9.4         | 32.7        |
|              | 0.6      | 50    | 20  | 0.9 | <b>11.2</b> | <b>37.3</b> | <b>9.3</b>  | 35.0        | 11.3        | <b>33.7</b> | 7.7         | 29.0        | 8.7         | 33.3        | 7.0        | 28.0        | 9.2         | 32.7        |
|              | 0.6      | 50    | 25  | 0.9 | 11.7        | 38.0        | 10.0        | 37.3        | <b>10.6</b> | <b>33.7</b> | 7.5         | 28.7        | <b>8.5</b>  | <b>31.3</b> | <b>6.5</b> | 26.3        | <b>9.1</b>  | 32.6        |
|              | 0.6      | 50    | 20  | 0.9 | <b>11.2</b> | 37.3        | <b>9.3</b>  | <b>35.0</b> | <b>11.3</b> | <b>33.7</b> | 7.7         | 29.0        | <b>8.7</b>  | 33.3        | 7.0        | 28.0        | <b>9.2</b>  | <b>32.7</b> |
|              | 0.6      | 100   | 20  | 0.9 | <b>11.2</b> | <b>36.7</b> | 9.9         | 35.3        | 11.8        | 36.0        | <b>7.4</b>  | 28.7        | 8.9         | 33.3        | <b>6.8</b> | 27.7        | 9.3         | 33.0        |
|              | 0.6      | 150   | 20  | 0.9 | 11.4        | 38.7        | 9.9         | <b>35.0</b> | 11.8        | 35.7        | 7.7         | 28.0        | 9.0         | 33.7        | 7.0        | <b>26.7</b> | 9.5         | 33.0        |
|              | 0.6      | 200   | 20  | 0.9 | 12.2        | 40.7        | 10.0        | 35.3        | 11.8        | 36.0        | 7.7         | <b>26.7</b> | 8.8         | <b>32.3</b> | 7.2        | 27.0        | 9.6         | 33.0        |

Table 18: Ablation studies on the hyper-parameters of SAVER with “*High*” early exit layers, including the number of candidate tokens  $k$ , the scale factor  $\alpha$ , the number of candidate image representations  $N_i$ , and the threshold  $p$ . CHAIRs and CHAIRi are denoted as Cs and Ci. Lower Cs and Ci indicate fewer hallucinations.

| Model        | $\alpha$ | $N_i$ | $k$ | $p$ | Cartoon     |             | Game       |             | Graffiti    |             | Painting    |             | Sketch     |             | Original   |             | Average     |             |
|--------------|----------|-------|-----|-----|-------------|-------------|------------|-------------|-------------|-------------|-------------|-------------|------------|-------------|------------|-------------|-------------|-------------|
|              |          |       |     |     | Ci          | Cs          | Ci         | Cs          | Ci          | Cs          | Ci          | Cs          | Ci         | Cs          | Ci         | Cs          | Ci          | Cs          |
| LLaVA-1.5    | 0.4      | 50    | 20  | 0.9 | 11.3        | 37.0        | <b>8.2</b> | <b>28.7</b> | <b>12.1</b> | <b>36.3</b> | 11.2        | 35.7        | <b>9.5</b> | 33.0        | <b>6.3</b> | <b>24.0</b> | <b>9.8</b>  | 32.5        |
|              | 0.6      | 50    | 20  | 0.9 | 11.3        | 37.0        | 8.3        | 29.7        | 12.3        | 37.3        | 11.3        | 33.3        | 9.8        | <b>32.3</b> | 6.7        | 25.3        | 10.0        | 32.5        |
|              | 0.8      | 50    | 20  | 0.9 | 10.8        | <b>33.3</b> | 8.3        | 29.3        | 13.2        | 38.3        | 11.1        | 33.3        | 10.6       | 35.0        | 7.4        | 28.3        | 10.2        | 32.9        |
|              | 1.0      | 50    | 20  | 0.9 | <b>10.7</b> | 34.3        | 8.5        | 30.0        | 13.5        | 39.0        | <b>10.6</b> | <b>31.3</b> | 10.4       | 35.3        | <b>6.3</b> | 24.7        | 10.0        | <b>32.4</b> |
|              | 0.6      | 50    | 20  | 0.6 | 10.5        | 35.0        | 9.1        | 29.3        | 12.6        | 38.0        | 11.1        | 35.3        | <b>9.6</b> | 33.7        | <b>5.6</b> | 25.0        | 9.8         | 32.7        |
|              | 0.6      | 50    | 20  | 0.7 | 10.7        | 34.7        | 8.8        | 31.3        | <b>11.5</b> | <b>35.3</b> | 10.1        | 34.0        | 10.7       | 36.3        | 5.9        | <b>22.3</b> | 9.6         | 32.3        |
|              | 0.6      | 50    | 20  | 0.8 | <b>9.9</b>  | <b>33.7</b> | 8.6        | <b>29.0</b> | 12.1        | 38.7        | <b>9.7</b>  | <b>31.3</b> | 10.6       | 35.0        | 6.1        | 23.3        | <b>9.5</b>  | <b>31.8</b> |
|              | 0.6      | 50    | 20  | 0.9 | 11.3        | 37.0        | <b>8.3</b> | 29.7        | 12.3        | 37.3        | 11.3        | 33.3        | 9.8        | <b>32.3</b> | 6.7        | 25.3        | 10.0        | 32.5        |
|              | 0.6      | 50    | 10  | 0.9 | 11.4        | 37.3        | 10.2       | 32.3        | 12.2        | <b>37.0</b> | <b>10.9</b> | 32.0        | 11.5       | 36.3        | <b>6.0</b> | <b>25.3</b> | 10.4        | 33.4        |
|              | 0.6      | 50    | 15  | 0.9 | <b>11.0</b> | 38.0        | 9.0        | 31.7        | 12.6        | 39.3        | <b>10.9</b> | <b>31.0</b> | 10.4       | 33.3        | 7.2        | 27.3        | 10.2        | 33.4        |
|              | 0.6      | 50    | 20  | 0.9 | 11.3        | <b>37.0</b> | <b>8.3</b> | <b>29.7</b> | 12.3        | 37.3        | 11.3        | 33.3        | <b>9.8</b> | <b>32.3</b> | 6.7        | <b>25.3</b> | <b>10.0</b> | <b>32.5</b> |
|              | 0.6      | 50    | 25  | 0.9 | 11.7        | 38.3        | 8.5        | 30.7        | <b>12.0</b> | 37.7        | 11.0        | 33.3        | 10.0       | 33.0        | 6.6        | 33.7        | <b>10.0</b> | 34.5        |
| MiniGPT-4    | 0.6      | 50    | 20  | 0.9 | 11.3        | <b>37.0</b> | <b>8.3</b> | <b>29.7</b> | <b>12.3</b> | 37.3        | 11.3        | 33.3        | <b>9.8</b> | <b>32.3</b> | 6.7        | 25.3        | <b>10.0</b> | <b>32.5</b> |
|              | 0.6      | 100   | 20  | 0.9 | 11.2        | 38.0        | 9.6        | 33.7        | <b>12.3</b> | 37.3        | 10.8        | 33.0        | 10.2       | <b>32.3</b> | 6.9        | 25.3        | 10.2        | 33.3        |
|              | 0.6      | 150   | 20  | 0.9 | <b>11.0</b> | <b>37.0</b> | 9.0        | 30.3        | 13.2        | 38.3        | 10.1        | 32.7        | 11.0       | 35.3        | <b>6.6</b> | <b>24.3</b> | 10.2        | 33.0        |
|              | 0.6      | 200   | 20  | 0.9 | 11.4        | 37.7        | 9.3        | 31.7        | 13.1        | <b>36.7</b> | <b>9.9</b>  | <b>32.0</b> | 10.6       | 34.0        | 6.9        | 25.3        | 10.2        | 32.9        |
|              | 0.4      | 50    | 20  | 0.9 | <b>9.2</b>  | <b>27.0</b> | 8.5        | 29.0        | 8.8         | <b>24.3</b> | <b>7.9</b>  | <b>25.0</b> | <b>7.7</b> | <b>24.0</b> | 6.0        | 25.0        | <b>8.0</b>  | <b>25.7</b> |
|              | 0.6      | 50    | 20  | 0.9 | 9.6         | 29.3        | 8.6        | <b>27.7</b> | <b>8.7</b>  | 25.0        | 8.4         | 25.7        | 8.0        | 27.0        | 6.6        | 26.0        | 8.3         | 26.8        |
|              | 0.8      | 50    | 20  | 0.9 | <b>9.2</b>  | 28.7        | <b>8.2</b> | <b>27.7</b> | 8.9         | 25.7        | 8.5         | 25.3        | 7.8        | 26.0        | 6.6        | 25.3        | 8.2         | 26.5        |
|              | 1.0      | 50    | 20  | 0.9 | 9.4         | 30.0        | 8.8        | 28.7        | 9.3         | 28.0        | 8.5         | 25.3        | 8.1        | 28.0        | <b>5.8</b> | <b>24.0</b> | 8.3         | 27.3        |
|              | 0.6      | 50    | 20  | 0.6 | 10.2        | 32.3        | 9.4        | 31.0        | 10.8        | 32.0        | 9.4         | 30.3        | 9.7        | 31.3        | 7.1        | 27.7        | 9.4         | 30.8        |
|              | 0.6      | 50    | 20  | 0.7 | <b>8.8</b>  | 29.7        | 9.4        | 30.7        | 10.0        | 27.7        | <b>8.4</b>  | 28.3        | 9.1        | 28.0        | 6.4        | <b>24.0</b> | 8.7         | 28.1        |
|              | 0.6      | 50    | 20  | 0.8 | 9.8         | 33.0        | 9.0        | 29.0        | 9.0         | <b>24.7</b> | 8.5         | 28.3        | 8.9        | 28.7        | <b>6.0</b> | 25.0        | 8.5         | 28.1        |
|              | 0.6      | 50    | 20  | 0.9 | 9.6         | <b>29.3</b> | <b>8.6</b> | <b>27.7</b> | <b>8.7</b>  | 25.0        | <b>8.4</b>  | <b>25.7</b> | <b>8.0</b> | <b>27.0</b> | 6.6        | 26.0        | <b>8.3</b>  | <b>26.8</b> |
| InstructBLIP | 0.6      | 50    | 10  | 0.9 | <b>9.2</b>  | 29.3        | 8.9        | 29.0        | 8.5         | 23.7        | 8.7         | 28.0        | <b>7.8</b> | <b>26.0</b> | <b>6.3</b> | <b>24.0</b> | <b>8.2</b>  | 26.7        |
|              | 0.6      | 50    | 15  | 0.9 | 9.4         | 30.3        | 8.5        | <b>27.0</b> | <b>8.2</b>  | <b>23.3</b> | 8.7         | 25.7        | 7.9        | 26.3        | 6.5        | 25.3        | <b>8.2</b>  | <b>26.3</b> |
|              | 0.6      | 50    | 20  | 0.9 | 9.6         | 29.3        | 8.6        | 27.7        | 8.7         | 25.0        | <b>8.4</b>  | 25.7        | 8.0        | 27.0        | 6.6        | 26.0        | 8.3         | 26.8        |
|              | 0.6      | 50    | 25  | 0.9 | 9.5         | <b>28.7</b> | <b>8.3</b> | 27.3        | 8.9         | 25.3        | <b>8.4</b>  | <b>25.0</b> | 7.9        | 27.3        | 6.6        | 26.0        | 8.3         | 26.6        |
|              | 0.6      | 50    | 20  | 0.9 | 9.6         | 29.3        | 8.6        | 27.7        | <b>8.7</b>  | <b>25.0</b> | <b>8.4</b>  | <b>25.7</b> | <b>8.0</b> | <b>27.0</b> | 6.6        | 26.0        | <b>8.3</b>  | 26.8        |
|              | 0.6      | 100   | 20  | 0.9 | <b>9.3</b>  | <b>28.3</b> | <b>8.4</b> | <b>26.7</b> | 8.9         | 25.7        | 8.7         | 26.3        | 8.1        | <b>27.0</b> | 6.7        | 26.0        | 8.4         | <b>26.7</b> |
|              | 0.6      | 150   | 20  | 0.9 | 9.4         | 28.7        | 8.7        | 28.3        | 8.9         | <b>25.0</b> | 8.8         | 26.7        | 8.5        | 28.0        | <b>6.5</b> | <b>25.3</b> | 8.5         | 27.0        |
|              | 0.6      | 200   | 20  | 0.9 | 9.8         | 29.0        | 8.7        | 28.0        | 8.8         | 25.3        | 8.8         | 27.3        | 8.2        | 27.7        | <b>6.5</b> | 25.7        | 8.5         | 27.2        |
|              | 0.4      | 50    | 20  | 0.9 | <b>11.0</b> | 32.7        | <b>7.8</b> | 25.7        | <b>9.6</b>  | <b>29.3</b> | <b>7.5</b>  | 24.7        | <b>7.0</b> | 24.7        | <b>6.1</b> | <b>21.7</b> | <b>8.2</b>  | <b>26.5</b> |
|              | 0.6      | 50    | 20  | 0.9 | 11.3        | <b>31.3</b> | 8.4        | 28.0        | 10.9        | 31.0        | 8.2         | 26.7        | 7.1        | 24.7        | 6.3        | 23.0        | 8.7         | 27.5        |
|              | 0.8      | 50    | 20  | 0.9 | 11.8        | 33.7        | 8.5        | <b>25.3</b> | 10.4        | 30.0        | 8.2         | <b>24.3</b> | 8.0        | 26.0        | 6.3        | 24.3        | 8.9         | 27.3        |
|              | 1.0      | 50    | 20  | 0.9 | 12.0        | 33.7        | 8.8        | 28.3        | 10.0        | 30.7        | 8.8         | 25.7        | 7.7        | <b>23.7</b> | 6.9        | 25.7        | 9.0         | 28.0        |
| InstructBLIP | 0.6      | 50    | 20  | 0.6 | 10.0        | 34.7        | 8.4        | 32.0        | <b>9.6</b>  | 30.7        | <b>8.0</b>  | 27.0        | 8.1        | 27.7        | 6.4        | 25.0        | 8.4         | 29.5        |
|              | 0.6      | 50    | 20  | 0.7 | <b>9.9</b>  | 32.0        | <b>7.5</b> | 29.0        | 10.3        | <b>29.7</b> | 8.4         | 25.7        | 7.2        | 27.7        | 5.8        | 24.7        | <b>8.2</b>  | 28.1        |
|              | 0.6      | 50    | 20  | 0.8 | 10.3        | 33.7        | 8.6        | 29.0        | 10.1        | <b>29.7</b> | 8.3         | <b>25.0</b> | 7.4        | 27.3        | <b>5.7</b> | <b>19.7</b> | 8.4         | <b>27.4</b> |
|              | 0.6      | 50    | 20  | 0.9 | 11.3        | <b>31.3</b> | 8.4        | <b>28.0</b> | 10.9        | 31.0        | 8.2         | 26.7        | <b>7.1</b> | <b>24.7</b> | 6.3        | 23.0        | 8.7         | 27.5        |
|              | 0.6      | 50    | 10  | 0.9 | 10.6        | 34.7        | 8.5        | 28.3        | <b>9.7</b>  | 29.7        | 8.8         | 27.3        | 8.4        | 30.3        | <b>5.9</b> | <b>20.0</b> | <b>8.7</b>  | 28.4        |
|              | 0.6      | 50    | 15  | 0.9 | 10.6        | 33.3        | 8.1        | <b>26.0</b> | 10.8        | 32.3        | <b>8.1</b>  | <b>26.3</b> | 7.8        | 28.7        | 6.5        | 32.7        | <b>8.7</b>  | 29.9        |
|              | 0.6      | 50    | 20  | 0.9 | 11.3        | <b>31.3</b> | 8.4        | 28.0        | 10.9        | 31.0        | 8.2         | 26.7        | <b>7.1</b> | <b>24.7</b> | 6.3        | 23.0        | <b>8.7</b>  | 27.5        |
|              | 0.6      | 50    | 25  | 0.9 | <b>10.5</b> | <b>31.3</b> | <b>8.0</b> | 26.3        | 9.9         | <b>27.0</b> | 9.4         | 28.0        | 7.7        | 25.7        | 6.4        | 23.7        | <b>8.7</b>  | <b>27.0</b> |
|              | 0.6      | 50    | 20  | 0.9 | 11.3        | 31.3        | <b>8.4</b> | 28.0        | 10.9        | 31.0        | <b>8.2</b>  | 26.7        | <b>7.1</b> | <b>24.7</b> | 6.3        | 23.0        | 8.7         | 27.5        |
|              | 0.6      | 100   | 20  | 0.9 | 10.7        | 30.0        | 8.5        | <b>27.0</b> | 10.3        | 29.3        | <b>8.2</b>  | <b>25.3</b> | 7.2        | 25.3        | 6.8        | 23.7        | 8.6         | <b>26.8</b> |
|              | 0.6      | 150   | 20  | 0.9 | 11.1        | 30.3        | 9.3        | 28.3        | 9.6         | 28.3        | 8.6         | 26.7        | 8.0        | 27.3        | 6.1        | <b>21.7</b> | 8.8         | 27.1        |
|              | 0.6      | 200   | 20  | 0.9 | <b>10.4</b> | <b>29.7</b> | 9.0        | <b>27.0</b> | <b>9.5</b>  | <b>27.7</b> | 8.3         | 27.7        | 7.9        | 27.3        | <b>6.0</b> | 22.0        | <b>8.5</b>  | 26.9        |



**Opera** : The image is a black and white drawing of a young boy sitting at a dining table. He is holding a knife and appears to be cutting into a loaf of bread. The table is set with various items, including a **bowl**, a **spoon**, and a **fork**.

**Deco** : The image depicts a young boy in a darkened room, sitting at a table with a plate of food in front of him. He appears to be eating something off of the plate, possibly a **sandwich** or a piece of **bread**. There are several utensils on the table.

**Ours** : The image depicts a boy in a darkened room, kneeling down next to a table. He is in the process of cutting something on the table using a knife. There are several knives present in the scene, one near the boy, another towards the table.

**Opera** : The image features a cat lying on top of a laptop keyboard, taking up a significant portion of the laptop's surface. The cat appears to be sleeping or resting comfortably on the keyboard. The laptop is placed on a **desk**, and the cat's presence adds a playful and cozy atmosphere



**Deco** : The image depicts a cat laying down on top of a keyboard, occupying most of the keyboard space. The cat appears to be sleeping or resting comfortably on the keyboard. In addition to the keyboard, there is a **mouse** located towards the right side of the keyboard.

**Ours** : The image depicts a cat laying down on top of a keyboard. The cat occupies most of the keyboard area, with its body occupying most of the space. The cat's positioning on the keyboard may cause some keys to be pressed unintentionally, but it seems content lay



**Opera** : The image depicts a person sitting at a dining table, enjoying a delicious pizza. The table is set with various items, including a **knife**, a **fork**, a **spoon**, a **bowl**, and cups. There are also apples placed on the table, adding variety to the

**Deco** : The image depicts a table setting with a delicious pizza prominently placed in the center of the table. The table is adorned with various utensils such as **knives**, **forks**, and **spoons** positioned around the pizza. There are also several bowls placed on the table

**Ours** : The image is a drawing depicting a table full of delicious food items. On the table, there is a delicious looking pizza prominently displayed, along with several apples scattered around. Additionally, there are two bowls placed on the table, one towards the left side and another towards the right

Figure 8: Qualitative results on LLaVA-1.5 using different decoding methods. Hallucinated objects are highlighted in red.



**Opera** : The painting depicts a woman in a white apron and green headscarf standing at a counter in a kitchen, holding a large pizza in her hand. The kitchen has a stainless steel **sink**, a gas **stove**, and a refrigerator in the background.

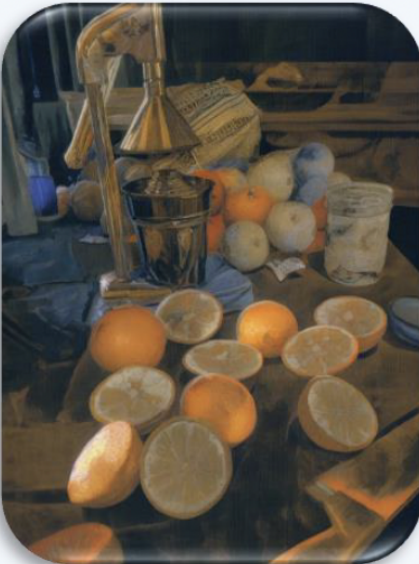
**Deco** : This painting depicts a woman in a white apron preparing a pizza in a kitchen. She is standing next to a counter with a pizza pan in her hands. The countertop is covered with ingredients such as **tomatoes**, **cheese**, and **sausage**.

**Ours** : This painting depicts a woman in a white apron and hat bending over a counter, preparing a pie. The background is green and there is a counter in the foreground. The woman's face is expressionless and her hair is in a bun. The pie in the foreground is green.

**Opera** : The image shows a table with various items on it, including a bowl of rice, a spoon, a **bottle** of water, and a piece of paper with writing on it. The background is a wooden table with a metal surface.

**Deco** : This image depicts a table with various items on it, including a map, a bowl of rice, a spoon, and a **cup of tea**. The table is outside, likely in a park or outdoor setting. The image is rendered in a realistic style with detailed textures and lighting effects

**Ours** : The image depicts a table with various items on it, including a pot of food, utensils, and a map. The pot of food appears to be a stew or soup, and the utensils include a fork, spoon, and knife.

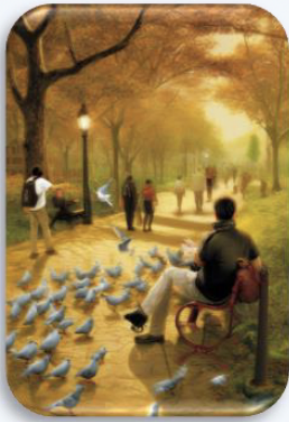


**Opera** : The painting depicts a table with several oranges sliced in half and placed on top of it. There is a metal bowl filled with oranges on the left side of the table, and a metal **pitcher** filled with water on the right side. The background is a dark, textured surface with.

**Deco** : This image depicts a table with a juice maker and several orange slices on it. The juice maker is made of metal and has a handle on it. There are also several other objects on the table, including a bowl and a **pitcher**. The tablecloth is patterned with

**Ours** : The image shows a table with several oranges and a juicer on it. The table is in a room with a window in the background. The juicer is made of metal and has a handle and a spout. The oranges are cut in half and are on the table in front of the.

Figure 9: Qualitative results on MiniGPT-4 using different decoding methods. Hallucinated objects are highlighted in red.



**Opera** : The image depicts a park scene with a man sitting on a bench surrounded by a flock of pigeons. The man is reading a **book**, and there are several other people scattered throughout the park, some walking and others sitting on benches or **chairs**.

**Deco** : The painting depicts a park scene where a man sits on a bench, reading a **book** while birds fly around him. The birds are in various positions in the painting, some flying overhead, others perched on benches or on the ground near the man. There are also several other people in the painting

**Ours** : The painting depicts a park scene with a man sitting on a bench in the center of the image. He is surrounded by birds, including several in the foreground and others further away in the background. The birds are in various positions, some perched on benches, others on the ground.

**Opera** : The image features a dining table with a white plate filled with various food items, such as bread, crackers, and a **bottle** of wine. There are also two glasses on the table, one on the left side and the other on the right side.

**Deco** : The image depicts a tabletop with a knife sticking out of a grill grate. The grill grate itself is in the center of the tabletop, with the knife sticking out of it. There are several utensils scattered around the tabletop, including a **fork**.

**Ours** : The image features a table set up for a meal, with a white plate displaying a variety of food items. There are several pieces of bread, including one in the center of the plate and others positioned near the edges. A wine glass is placed near the center of the table, and there are two additional wine.



**Opera** : The image depicts a cluttered room filled with various items, including a chair, a **table**, and a **couch**. There are also several potted plants scattered throughout the room, adding to the overall cluttered atmosphere. A window can be seen in the background, providing some natural light to the space.

**Deco** : The image depicts a room full of cluttered and cluttered items, including a **table**, chair, and various objects such as pots and pans, pots, and pans. There are several pots and pans scattered around the room, some of them positioned near the table.

**Ours** : The image depicts a cluttered and messy room with a variety of items strewn about. There are several potted plants in the room, including one near the window, another near the left side of the room, and another near the right side of the room. A chair can be seen in the.

Figure 10: Qualitative results on InstructBLIP using different decoding methods. Hallucinated objects are highlighted in red.